SAPIENZA
UNIVERSITÀ DI ROMA

FACOLTÀ DI INGEGNERIA CIVILE E INDUSTRIALE

Corso di laurea magistrale in Ingegneria Civile

PERFORMANCE BASED ASSESSMENT OF A NEW PRECAST MODULAR SYSTEM

Laureando:
Alyssa Di Campli

Relatore: Prof. Ing. Paolo Franchin

Correlatore: Prof. Ing. Andrea Lucchini

Correlatore esterno: Prof. Doctor André Furtado

A.A. 2024-2025

SAPIENZA
UNIVERSITÀ DI ROMA

Performance based assessment of a new modular precast system

Facoltà di Ingegneria Civile e Industriale
Dipartimento di Ingegneria Strutturale e Geotecnica
Corso di laurea in Ingegneria Civile

Alyssa Di Campli
Matricola 1903999

Relatore
Prof. Ing. Paolo Franchin

Correlatore
Prof. Ing. Andrea Lucchini
Prof. Ing. Andrè Furtado

A.A. 2024-2025

Ai miei nonni,

Mamou, Papou, Nonna Maria e Nonno Mario,

mia luce e esempio di amore

TABLE OF CONTENTS

LIST OF FIGURES

LIST OF TABLES

ACKNOWLEDGEMENTS

Throughout the course of writing this dissertation, I have been grateful for the unwavering support and guidance I have received.

I would like to begin by expressing my sincere gratitude to my supervisors, Professor Paolo Franchin, for given me this opportunity and for the trust he placed in me, as well as for shearing his immense expertise, the Professor Andrea Lucchini for his support during my most challenging times, and Professor Andrè Furtado, who has supported me throughout the development of this study and has always been so kind and understanding. I will never forget his dedication to my work; he always found time to help me despite the distance. I have learned a lot not only in the scientific field but also in terms of personal growth and development.

A sincere thank you goes to my university colleagues: Ludovica, Lorenzo, Caterina, Elena, Gaetano, Giuseppe, Luca, and Marco. Thank you all for making these years of study such a unique experience, filled with unforgettable memories.

Thank you also to all my friends Arianna, Beatrice, Francesca, Irene and Martina, as well as, Gloria, Guglielmo, Nicoletta and all my "Viaggio" friends for their genuine friendship and for always being there to support.

Finally, I would like to express my heartfelt thanks to my family for giving me the opportunity to study, and for their constant support and encouragement. I truly hope I have made you proud.

I would also like to thank all those who have shared even a small part of this journey with me, no achievement would truly matter without all of you by my side.

ABSTRACT

This study examines the seismic performance of a specific prefabrication concept patented in Portugal with the project named "R2UTechnologies Modular Systems". The design of this system is not conceived from inception to resist large lateral forces. Consequently, the prefabrication industry is prevented from fully exploiting its potential and from expanding into markets located in seismic-prone regions.

The studied building adopts a wall-based structural system with reinforcing bars and dry-bolted connections between structural elements. To assess the system, nonlinear static pushover and nonlinear dynamic analyses were performed on a small-scale building, devised specifically for this thesis. This smaller model, more manageable yet representative of all system characteristics. The results provide insight into the mechanisms governing the seismic behaviour of the proposed wall system. For the full-scale building, only a nonlinear static analysis was conducted to evaluate its seismic performance under different seismicity conditions.

In conclusion, the analyses demonstrate that the lateral capacity of the system is primarily governed by interface sliding, while the shear connections in the vertical interfaces play a secondary role. Despite the prevalence of sliding mechanisms, displacements remain limited, confirming compliance with relevant performance requirements. These findings suggest that the system can achieve satisfactory seismic performance, and highlight avenues for future development, including the optimization of frictional interfaces and the potential implementation of energy-dissipating connections.

The study supports the development of reliable modelling guidelines for precast modular wall systems and contributes to a better understanding and improvement of their seismic behaviour and assessment.

Nota del Relatore. Senza che questo rappresenti assolutamente un giudizio in un senso o nell'altro su questa specifica tesi, devo avvertire che il testo finale della stessa, come di tu◎e le altre che ho seguito e seguirò, può non essere completamente soddisfacente da un punto di vista linguistico. Come docente universitario di Tecnica delle costruzioni non posso sostituirmi, in fase di supervisione di una tesi, a un intero percorso scolastico precedente. Devo necessariamente limitarmi a indirizzare sul piano tecnico e in questo ambito cercare di individuare, nel tempo limitato che a ogni tesi può essere dedicato, eventuali errori, che possono purtroppo comunque sfuggire.

1 INTRODUCTION

1.1 CONTEXT

Precast concrete represents a highly developed construction methodology that has evolved over the last century. Originating in Europe and gaining global adoption, it allows the production of structural elements in controlled factory conditions, ensuring high dimensional accuracy, control quality, faster construction, reduced workmanship and efficient use of materials. The method enables accelerated on-site assembly, reduces construction waste, and provides opportunities for modular and repeatable designs, making it increasingly popular in both commercial and residential projects [1].

fib's documents affirm that connections are the most crucial parts of a precast structure, and their performance is associated with structural limit states, manufacture, assembly and maintenance of the structure itself. The secret to producing a successful prefabricated structure resides in the adequate design of connections [2].

The use of precast concrete elements in seismic areas is considered a challenging task, mainly due to their structural behaviour under earthquake loading. Past events, such as the inadequate response of precast industrial buildings during the Emilia-Romagna earthquake in 2012, have highlighted the vulnerability of these systems [3].

1.2 OBJECTIVES AND NOVELTY

Investigations of precast structures affected by recent earthquakes have shown that connections are highly susceptible to severe damage. This vulnerability has prompted the development of numerous numerical models, ranging from macro-

scale [4], [5] to more detailed approaches [6], [7] aimed at simulating structural behaviour under seismic loading. However, due to their complexity, these models are often impractical for routine engineering design or seismic performance evaluation [3]. Consequently, there remains a pressing need to develop reliable numerical models for precast structures to support safer and more efficient structural design. In this context, the main objective of the present work is to perform a numerical performance assessment of a new developed precast modular wall system. The system is based on load-bearing walls and hollow-core slabs, which are interconnected through bolted connections. To achieve this the research proposes a numerical modelling approach capable of simulating the behaviour of insulated load-bearing walls, the performance of bolted connections at both vertical and horizontal interfaces, and the interaction between slabs and walls. The study is carried out with a progressive level of detail, starting from the local scale of the connections and extending to the global response of the entire structure.

1.3 STRUCTURE OF THE THESIS

The thesis begins with Section 1 which introduces the research context, the main objectives, and the novelty of the work, and provides an outline of the thesis structure. Section 2 reviews the state of the art, focusing on relevant literature concerning precast concrete systems in seismic areas and performance. Section 3 presents the case studies, describing the proposed modular precast wall system, its main components, experimental subassemblies, and the definition of a small building employed for nonlinear analysis calibration. Section 4 outlines the numerical modelling strategies adopted for walls, connections, and slabs. Section 5 presented the validation of the experimental tests on vertical connections through numerical modelling. Section 6 reports the analysis of the small

building, including modal analysis, nonlinear static pushover, and nonlinear dynamic simulations, complemented by sensitivity and parametric studies. Section 7 provides the performance assessment of a full-scale building in accordance with Eurocode 8 [8] considering different seismicity levels. Finally, Section 8 draws the main conclusions of the work and outlines possible directions for future research.

2 STATE OF THE ART

The purpose of this Section is to provide an overview of the current state of knowledge regarding precast concrete systems, with a particular focus on load-bearing wall structural systems and their connections. A comprehensive review of the literature is essential to identify the strengths and limitations of existing solutions, as well as to highlight the gaps that motivate the present research.

2.1 SEISMIC PERFORMANCE OF PRECAST CONCRETE STRUCTURES

Post-earthquake damage surveys can generally be classified into two main categories: structural and non-structural damage. In the following subsection, principal structural damages will be described and analysed, along with the parameters influencing seismic response and building load capacity. It is worth noting that modular precast concrete buildings in seismic regions are relatively rare worldwide, which has made it particularly challenging to obtain detailed information on this typology. Nevertheless, even though the available studies primarily focus on prefabricated industrial buildings, the observed damage patterns can serve as valuable references for assessing and improving the resilience of factory-built modular concrete structures [9].

The number of precast concrete buildings constructed with load-bearing wall systems in seismic regions is extremely limited, and, to date, no reports of earthquake-related damage have been documented for this structural typology. The most frequent structural damages observed during intense seismic activities were registered in columns, beams and several connections between elements such as beam-to-column, roof-to-beam, columns-to-foundation and cladding panel-to-structural elements [9].

2.1.1 Columns

Columns can experience different types of damage, including: (i) the formation of a plastic hinge at the base, (ii) short-column failure, and (iii) failure at the top. Among these, the most frequently observed damage in precast columns is the development of a plastic hinge at the base. Liberatore et al. [10] reported that more than 40% of the buildings investigated after the 2012 Emilia earthquake exhibited this type of failure. The origin of such damage is still debated: while some authors consider it a common structural issue, others argue that plastic hinge formation is not only related to inadequate column cross-sections (Casotto et al. [4]) but also to deficient design of beam-to-column connections. Figure 1 shows an example of a plastic hinge at the column base, whereas Figure 2 illustrates the buckling of reinforcing bars in compression.

Figure 1 Formation of a plastic hinge at the base of a column (Figure adapted from [10])

Figure 2 Buckling of longitudinal rebars at the base of the column (Figure adapted from [10])

Another type of damage associated with columns failure is the short-column effect. This phenomenon is caused due the arrangement of infill panels, adjacent to the precast concrete columns without an adequate seismic joint, contiguous halls with different weight (Figure 3) or sawtooth roofs with inclined beams. Indeed, the most frequent cause related with short-column is connected with industrial buildings with strip windows on top of curtain masonry walls/cladding panels [9].

Figure 3 Short column effect derived from presence of the masonry infill walls (Figure adapted from [9])

Finally, the top of the columns, local damages are common. According Liberatore et al. [10] there are two types of column top damages: i) spalling of the concrete that is directly supporting the beam; ii) failure of the lateral cantilever that restraints the pocket supports (Figure 4**Errore. L'origine riferimento non è stata trovata.**). The first type of damage, which can be related to exceedingly thick fire-protection cover concrete, and to the lack of a rubber interface between the concrete elements, is seldom critical, unless coupled with the beam sliding. On the contrary the second damage mode is frequently associated to the beam unseating. The connection between the two lateral restraints and the beam head may reduce the bending moment at the base of the pocket support walls and hamper the unseating of the beam [10].

Figure 4 Failure of lateral restraints of the pocket support. (Figure adapted from [10])

2.1.2 Beams

About beam seismic damages, in comparison to what has been extensively documented for other structural elements, beam failures are relatively uncommon. When they do occur, the primary cause is the loss of support. The

absence of a proper column-to-beam connection, which could also prevent the spalling between the column and the beam, is the main reason of the beam collapses [11].

Other problem associated with beams are is the beam rotation, as illustrated in Figure 5. This problem is associated with roof cladding panels, more specifically with the lack of connection. In many cases the collapse of the roof panels is a consequence of the beam failure. The study developed by Bournas et al. [11] reported that 25% of precast industrial buildings designed with no seismic provisions presented partial or total collapse of the roof and girders [11].

Figure 5 Out-of-plane counterclockwise rotation of the shed beam, and clockwise rotation of the cladding panel (Figure adapted from [10])

2.1.3 Connections

In a precast concrete building, structural connections represent a fundamental component of the overall load-resisting system. The global seismic performance is strongly influenced by the behaviour and mechanical characteristics of these

connections [2]. The connections that reach high levels of damage are typically beam-to-column, roof-to-beam, column-to-foundation and cladding panel-to-structural member.

During the Emilia earthquake in 2012, the most critical structural damages registered were associated with partial or total collapse of the roof, mainly due to the loss of seating of the main girder [11]. The research highlighted a significant example of inadequate beam-to-column connections, which resulted in the loss of support for the roof elements. The main challenge lies in ensuring that these connections possess sufficient capacity to accommodate relative displacements while maintaining beam seating, allowing for the proper transmission of horizontal forces from the beam to the column and subsequently to the foundation, all without compromising the overall structural performance [11].

The most common used roof systems are the flexible roofs and since these do not have any mechanical joint links, the seismic loads are directly transferred to the primary beams. However, this way the forces can surpass their out-of-plane capacity and collapse. Figure 6 shows damage to a beam as a result of inadequate beam-to-roof connection.

Figure 6 Inappropriate beam-to-roof connection (Figure adapted from [9])

Precast concrete structures are very sensitive to seismic events and connections between horizontal and vertical structural elements are the critical zones that may lead to collapse. So, the resistance of these structures under earthquake actions depends strongly on the performance of the connections present in the joints which means these joining elements need to be properly designed to maintain the integrity of the structure, in the most diverse range of parameters such as energy dissipation, strength and ductility [12].

Precast concrete construction for seismic applications can generally be classified into two types, emulative and jointed. In emulative construction, the connections are designed and detailed to ensure that the overall structural performance (in terms of lateral strength, stiffness, and energy dissipation) closely resembles that of an equivalent, conventionally designed, and properly detailed cast-in-place monolithic reinforced concrete structure. Capacity-design principles are typically adopted so that strong connections remain essentially in the linear-elastic range, while plastic hinges fully develop elsewhere in the structure. Conversely, jointed construction (also referred to as non-emulative detailing in the literature) uses precast connection concepts that are distinctly different from emulative

connections. In this approach, the nonlinear rotations of the structure are intentionally concentrated at the ends of the precast members within the joint regions This is achieved through controlled rocking mechanisms at the joint interface, allowing the dissipation of seismic energy while minimizing inelastic damage to the members themselves [13].

2.2 MODULAR PRECAST WALL SYSTEM

Precast wall systems are typically manufactured using reinforced concrete and are widely applied in both internal and external walls, as well as in functional components such as lift shafts and central cores. This construction method is most adopted in domestic buildings, where precast walls can serve either as load-bearing or non-load-bearing elements. Load-bearing precast walls play a fundamental structural role, as they transfer vertical and lateral loads to the foundation, ensuring both stability and strength of the overall system. Beyond their structural function, precast walls provide several additional benefits, including rapid construction, smooth surface finishing, good acoustic insulation, and inherent fire resistance [11].

Figure 7 Load-bearing wall structures (Figure adapted from [11])

Different construction solutions will be presented and discussed, such as plain walls, sandwich insulated walls and double wall, each with its own specific characteristics and purposes (Figure 8).

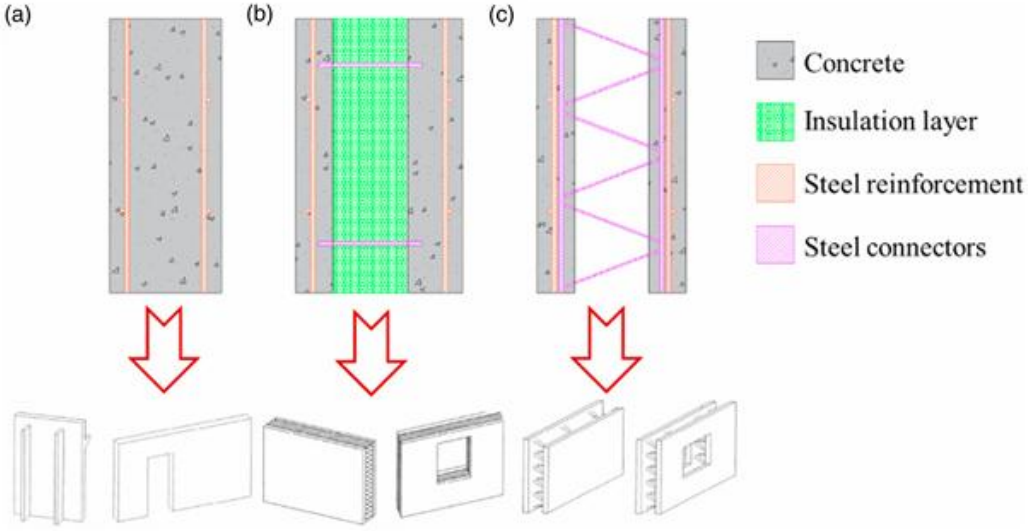

Figure 8 Types of precast wall according to the type of cross-section: (a) plain wall; (b) insulated wall; (c) double wall (Figure adapted from [14])

2.2.1 Plain wall

Plain walls represent the simplest type of precast wall system, composed of a single layer of concrete reinforced with steel. Their thickness typically ranges from 80 mm to 240 mm, making them a practical solution for a wide variety of construction applications. Thanks to their straightforward configuration, plain walls are the most adopted solution in current precast practice. They offer significant advantages in terms of factory production, being easier and more cost-effective to manufacture, while also allowing rapid installation on site [14].

Figure 9 Plain walls (Figure adapted from [14])

Reinforced concrete (RC) structural walls, play a crucial structural role, particularly in high-rise apartment buildings, where they are required to sustain substantial gravity and lateral loads. These walls often include different types of openings: small ones for machine and electric boxes, medium-sized openings for water pumps, and larger ones for windows and doors, all of which influence the overall structural behaviour [15].

The use of reinforced concrete structural walls is common for resisting lateral forces imposed by wind or earthquakes. In regions of high seismic risk, it is generally not feasible to design such walls to remain elastic during strong earthquakes; instead, inelastic deformations are expected, usually concentrated at the wall base. To ensure stable inelastic performance, however, careful detailing is required, particularly with the provision of adequate transverse reinforcement in regions subject to high strain demands [16].

2.2.2 Precast concrete sandwich panel (PCSP)

These panels were developed more than 70 years ago to overcome the thermal insulation shortcomings of solid precast concrete panels [17]. As depicted in

Figure 10, an insulation layer is sandwiched between two concrete layers and connected using mechanical shear connectors to form a three-layered sandwich panel [17].

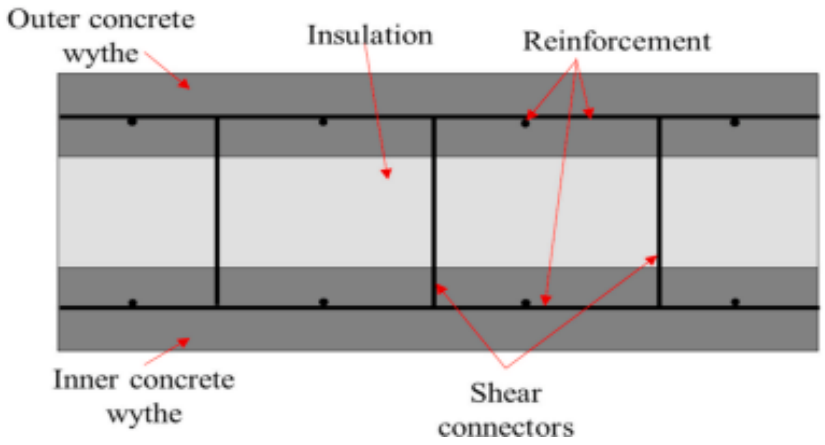

Figure 10 Precast concrete sandwich wall panel (Figure adapted from [17])

Originally adopted in low-rise industrial buildings, they are now increasingly used across a wider variety of building types, including mid to high-rise residential and commercial structure [18].

The main advantages of sandwich panels include rapid construction, good acoustic insulation, inherent fire resistance, and smooth interior surfaces that are ready for painting. However, these benefits come with certain limitations, such as reduced flexibility in layout and lower adaptability of the structural system. Typically, floors span in the longer direction, while for integrally precast wall systems, spans can be arranged in different orientations, though the most efficient solution is to align them in parallel [19].

Examples of PCSPs used in load bearing (VPC) and non-load bearing (NVPC) prefabricated buildings are shown in Figure 11.

a)  b) 

Figure 11 Prefabricated buildings using PCSPs (a) VPC, (b) NVPC. (Figure from [17])

The sandwich panels are lighters than the other panels, which enables them to be utilised in high importance buildings such as laboratories and hospital operating theatres [17].

Compared to traditional beam-and-column frames, precast sandwich panels generally exhibit greater stiffness. While this characteristic can limit architectural flexibility, it also provides significant advantages in seismic regions, where higher lateral resistance is beneficial for reducing damage and improving overall structural performance.

2.2.3 Double wall or pre-walls

The pre-walls system is characterized by two prefabricated concrete panels, connected by steel trusses (Figure 12). These modules, after being produced in factory and transported to construction site, are assembled, reinforcement is placed in critical regions, and the core is casting. The pre-walls are used as formwork for casting the concrete core, contributing to a cleaner construction site without formworks, and are also used as part of the structural wall, supporting part of the applied loads [20].

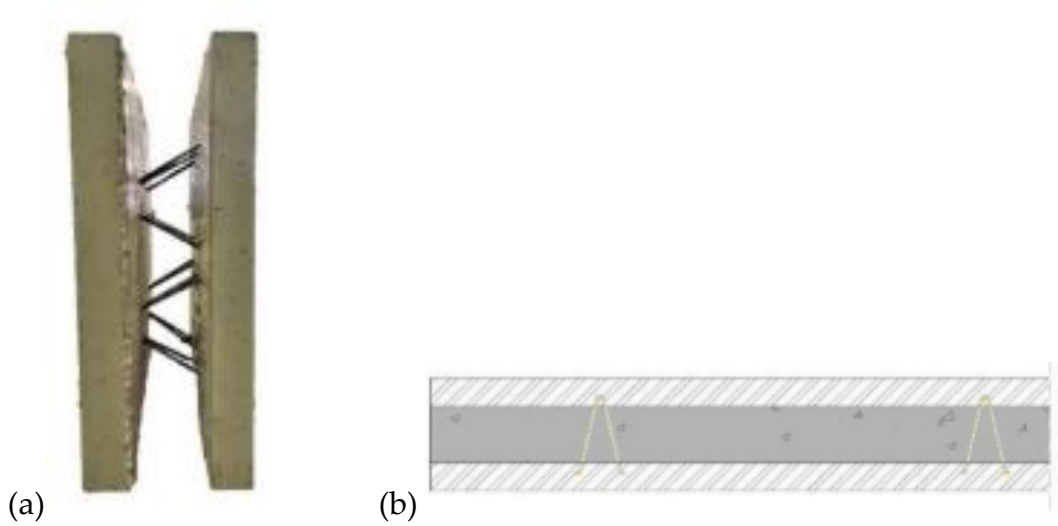

Figure 12 Pre-wall system: a) pre-wall made with UHDC; b) composite UHDC-concrete pre-wall (Figure adapted from [20])

An important development of this system is the *super-skin* concept, which incorporates ultra-high durability concrete (UHDC) in the prefabricated panels, i.e., in the outer layer of the wall, where maximum protection against environmental exposure is required. The core, by contrast, can be produced with lower performance concrete, allowing for a more economical use of materials. However, the structural performance and durability of these members strongly depend on the bond between the two concretes. Ensuring adequate interface strength is therefore a crucial requirement for the proper behaviour of the composite system [20].

2.3 CONNECTION BETWEEN PRECAST ELEMENTS

Connections between precast elements represent the most critical zones of a structure, as they are essential to ensure its overall integrity and seismic performance [21]. The primary function of the connections is to allow horizontal forces, such as a seismic action or wind, to be transferred for each element in the system, enabling a structural interaction, for the forces to reach the foundation. The connections must be designed considering not only the safety requirements,

i.e. to support the applied loads, but also the transport and assembly requirements. The connections between precast members can be classified as wet or dry, based on method applied [14].

2.3.1 Dry connections

Dry connections refer to mechanical couplers, such as steel plates, dowels, or bolts, which are used to assemble precast concrete members into a unified structure without relying on cast-in-place concrete to strengthen the joint. The adoption of these systems significantly accelerates construction processes, mainly because on-site casting is minimized. Moreover, dry connections enable easier disassembly and replacement of elements when required, which makes them a more sustainable alternative compared to traditional wet joints [22].

This chapter is focused on presenting various types of dry connections currently in use to connect precast concrete walls, together with their areas of application, highlighting both their advantages and limitation.

Unbonded post-tensioned prestressed and hybrid conditions were studied by different authors to connect precast concrete walls. Figure 13 shows an unbonded post-tensioned precast concrete wall with a rocking connection to the foundation base, named as the Single Rocking Wall (SRW). Under seismic lateral loads, the bottom corner of the SRW uplifts as the wall experiences a rocking motion. Seismic shear forces are transferred from the wall to the foundation through friction and the post-tensioning (PT) force enhances re-centering of the wall, following a seismic excitation [23].

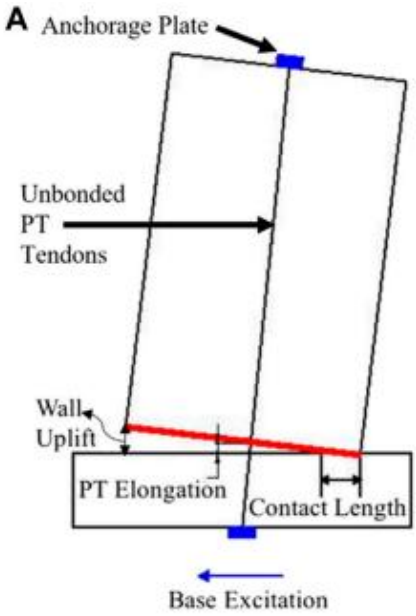

Figure 13 System setup: Single rocking wall (Figure adapted from [23])

These unbonded tendons consist of prestressed steel cables that are anchored and stressed individually, which can move freely relative to the concrete. Each tendon constitution is based on cables of high strength steel that are shielded through a corrosion-preventing coating and enfolded on a plastic casing. Nowadays, the practice of forming groups of several strands, wrapped each one individually, yet encased all together has been very popular in Europe [21].

With this method, the deformation of the structure remains in the elastic phase while the plastic deformations concentrate at the interfaces of the wall slab and so any problem that arises is easily fixed in comparison to a monolithic structure. The two kinds of deformations that can occur are shear slip in the horizontal intersection, which must be avoided by design, and gap opening (the expected deformation mode) [24]. Additionally, the tendons are capable by themselves of reducing deformation caused by a seismic event [21].

To improve the hysteretic damping of single rocking walls, different wall systems have been developed utilizing supplemental damping devices. For example, Priestley et al. [25] developed the jointed wall system where two or more precast concrete walls are connected horizontally with special stainless U-shaped Flexural Plates (Figure 14). Though adequate hysteretic damping can be provided through the UFPs, the jointed wall system has not found its way to practice because it provides reduced moment capacity compared to monolithic reinforced concrete walls and the fabrication of UFPs is uneconomical [23].

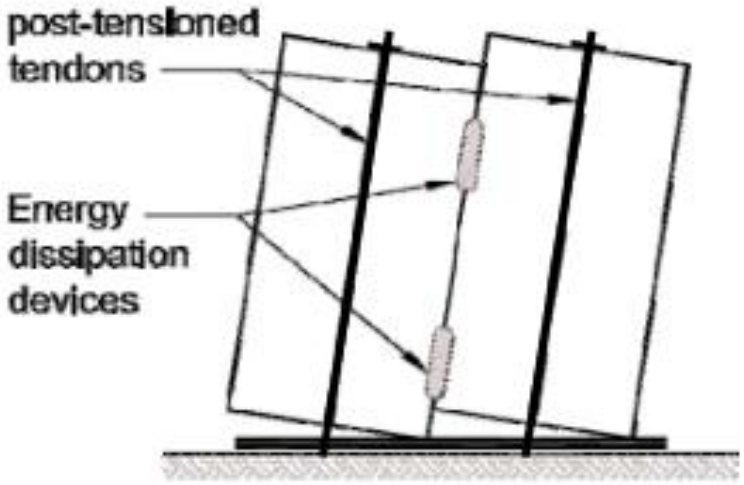

Figure 14 Jointed precast "hybrid" wall system: precast concrete walls connected with U-shaped Flexural Plates (Figure adapted from [26])

More recently, externally located and potentially replaceable dissipaters have been developed and experimentally validated, with the aim to further simplify the constructability and reparability of the structure after an earthquake event. This option would give the possibility to conceive a modular system with replaceable sacrificial fuses at the rocking connection, acting as the "weakest link of the chain", according to capacity design principles [26].

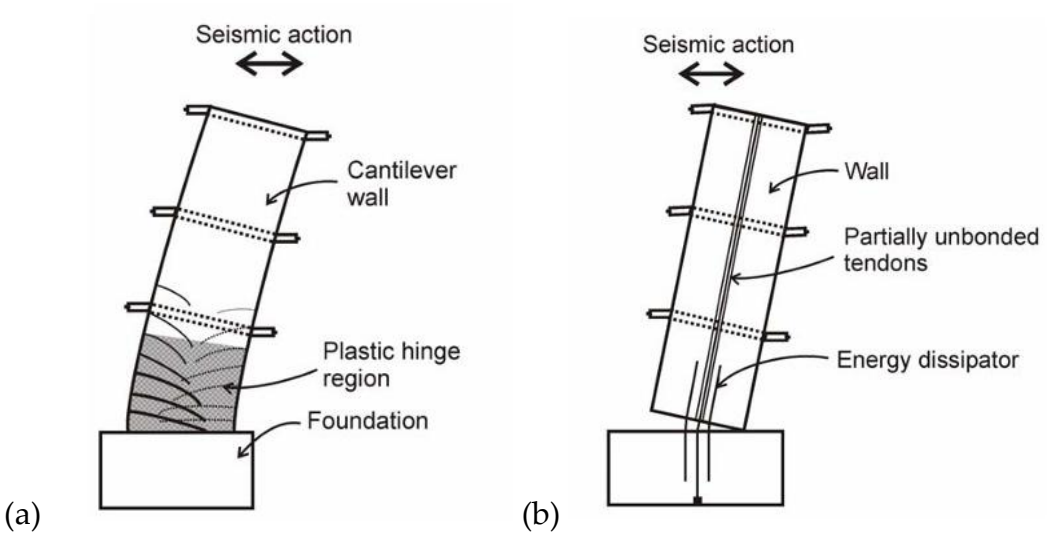

Figure 15 Comparative response: a) traditional monolithic system (damage in the plastic hinge) b) jointed precast (hybrid) solution (damage limited to the fuses and negligible residual deformations) (Figure adapted from [26])

The most pragmatic approach to dry connections involves the construction of entire structures composed of prefabricated walls joined by means of conventional or high-strength bolts. This technique allows for rapid assembly, does not requires casting (reducing the environmental impact), and has been widely adopted in steel construction [27]. However, there are still many topics that need to be overcome such as preventive measures for fire and rust and issues related to the screw fastening to guarantee a safe and reliable structure [21]. An example of this technology is a precast concrete structure connected entirely with bolts that was studied by Trivana et al. [21] of diverse technical details at the work site. The structure is organized into 4 block systems: a roof system, a wall system, a floor slab system, and a cushion block system (Figure 16). The precast wall system plays the role of load-bearing and lateral force resistance [21].

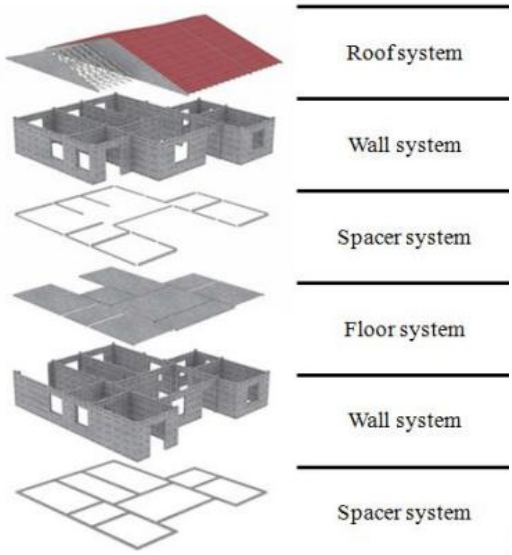

Figure 16 Total bolt connection prefabricated concrete structure (Figure adapted from [21])

Among the various types of bolted connections employed in precast structures, let us emphasize a precast concrete (PC) wall panel building system with bolted connections proposed by Zhao et al. [28]. In this system, the bolted joints were specifically designed to resist either tensile forces, shear forces, or a combination of both. As illustrated in Figure 17 the authors developed a lightweight precast panel system, consisting of thin, lightly reinforced panels connected through simple bolted joints. [28]

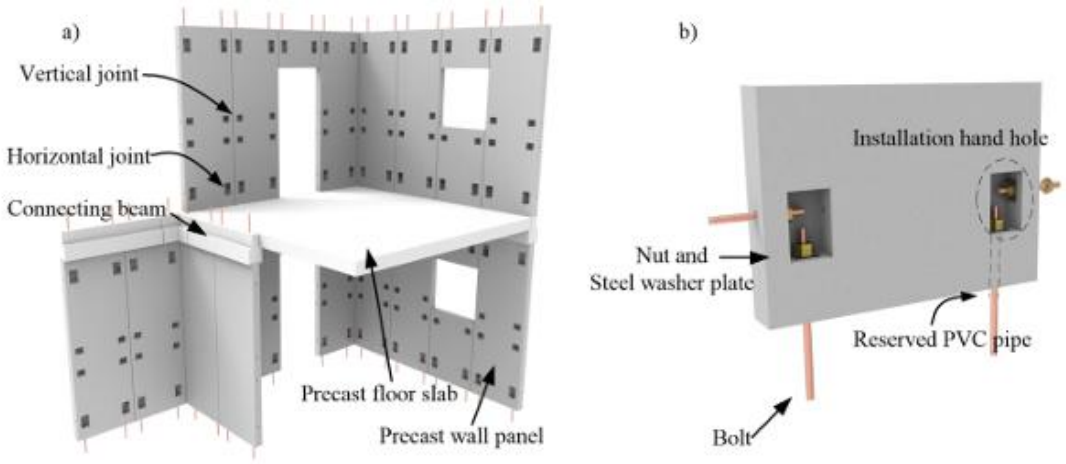

Figure 17 Bolted PC panel building system: (a) typical configuration, (b) post-installed bolted connection. (Figure adapted from [28]

The seismic performance of this system was assessed through quasi-static tests and finite element analyses (FEA), aimed at evaluating the structural response and identifying failure modes. The study also examined the influence of key variables such as axial load, concrete strength, aspect ratio, bolt diameter, number of bolts, and joint configuration [28]. The idealized force transfer mechanism and the failure mode of the bolted shear walls are schematically illustrated in Figure 18.

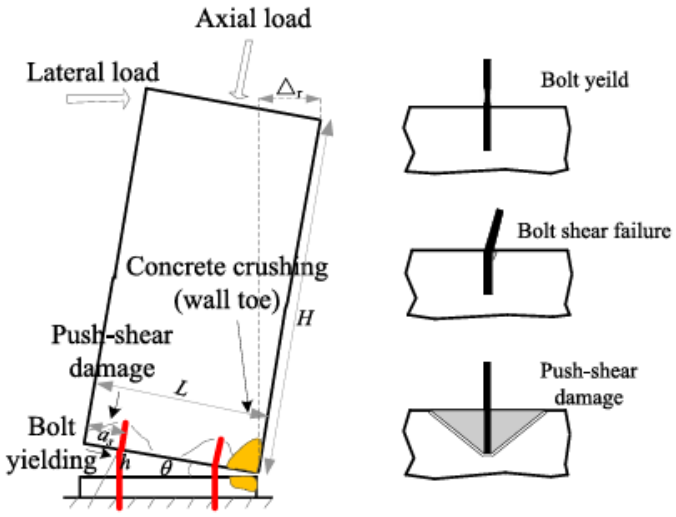

Figure 18 Failure and deformation mode of the bolted panels. (Figure adapted from [28])

Another example of dry connections for precast walls is the socket connection investigated by Acharya et al. [29] in their study on the seismic performance of full-scale modular structural concrete insulated panels (MSCIP) cantilever shear walls. Unlike conventional wall-to-footing connections that rely on starter bars, this system employs an innovative socket connection designed to enhance construction tolerances and significantly improve erection speed [29].

Figure 19 Integration of MSCIP wall specimen into a socket connection: socket footing wall connection (Figure adapted from [29])

Socket footings were employed to connect the prefabricated panels within a precast construction system. Full-scale prototypes were subjected to quasi-static cyclic loading, and the experimental results confirmed both satisfactory strength and ductility. However, the study highlighted the embedment length of the socket as a critical design parameter: when the embedment was insufficient, failure was dominated by anchorage mechanisms rather than the intended flexural behaviour. This finding underlines the necessity of providing adequate embedment length to ensure a ductile and reliable seismic performance [29].

Most of the dry joints using bolts may induce local concrete failure (cone breakout), but their performance is notably enhanced with the inclusion of steel plates. Accordingly, another type of bolted connection is the bolted steel plate horizontal joint, which employs two C-shaped steel plates bolted onto the flanges at both ends of the precast concrete wall as can be observed in Figure 20 [30].

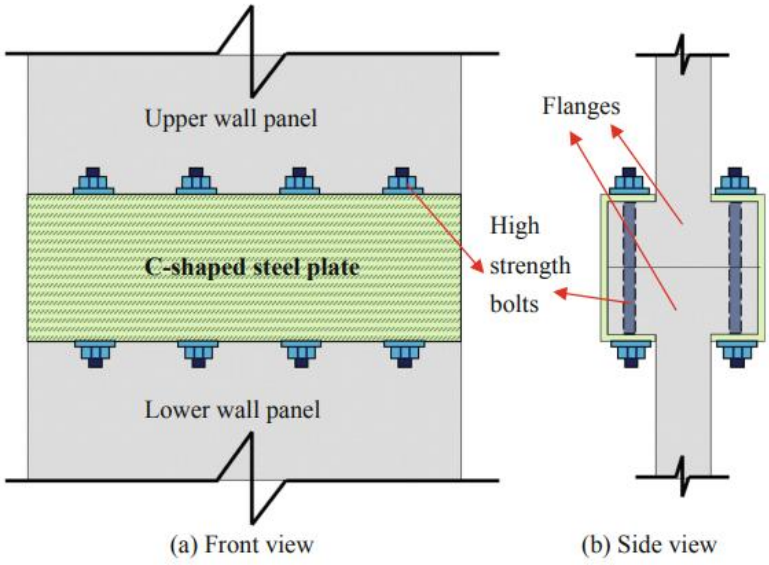

Figure 20 Bolted steel plate joint of precast shear wall: a) front view b) side view (Figure adapted from [30])

With this solution, concrete damage is expected to be primarily confined to the flanges, thereby preserving the integrity and safety of the main structural elements. Based on the findings of this research, it has emerged that using steel plates with slots, particularly horizontal slots, is preferable, as they significantly enhance the energy dissipation capacity of the bolted steel plate joints [30].

2.3.2 Wet connection

In general, wet connections concern the process of initially welding or coupling precast steel bars mechanically and generally uses cast-in-place concrete or grout of higher grade to fill the joint [31]. Therefore, a satisfying working system is

guaranteed through the transmission of the internal force of the longitudinal steel bars by the fusion of rebars and the mortar injected. This sort of connection manages the precast structures to achieve similar seismic performance as monolithic structures, also known as cast-in-place concrete structures. Nonetheless, there are some contrast associated with this method of attachment such as the increase of construction time due to the pouring of the concrete and subsequent curing and hardening, the excessive costs of steel sleeves and the uncertainty of ensuring the quality of the grouting operation [32].

Although this dissertation focuses on dry connections in precast concrete walls, three types of wet connections are also introduced. The first two types presented are used to link entire precast concrete elements, whereas the third one specifically refers to slab-to-slab connections.

1. **Steel sleeve grouting connection**

The sleeve grouting connection technology is to insert prefabricated steel bars into a steel sleeve and then pour high-strength grout into the sleeve. After the grout has set, the steel bars are strongly connected to the sleeves, ceding their force via bonding, friction and bite force. Sleeve grouting connection (Figure 21) can be prefabricated in the factory to simplify the construction process, but the relatively high cost of the sleeve, high requirements for processing accuracy, and high processing difficulty have also restricted its usage spectrum in engineering [21].

Figure 21 Sleeve grouting connection (Figure from [21])

There are two main types of steel sleeve grouting connections: full sleeve grouting and half sleeve grouting. The full sleeve connection is grouted at both ends, making it highly versatile and widely used. In contrast, the half sleeve connection consists of a straight-thread connection that is grouted on-site during assembly. Despite its shorter anchorage length and smaller size, the half sleeve connection tends to be more expensive due to the need for higher-quality sleeves and stricter reinforcement specifications [33].

An alternative and innovative configuration has been proposed to connect the upper and lower wall panels in precast concrete shear walls. As illustrated in Figure 22, the vertical reinforcing bars are intentionally discontinued in the mid-height region of the wall, while steel sections are embedded at the wall ends to strengthen the boundary elements. The connection between panels is achieved through grouted sleeves that anchor these steel sections, using conventional grouting materials to ensure adequate continuity between the precast elements. This grouted sleeve system, incorporating steel sections, offers several advantages, including high fault tolerance, reduced on-site workload, and improved alignment accuracy. Furthermore, the steel sections can be easily

positioned within the sleeves and provide enhanced robustness against construction-related disturbances [34].

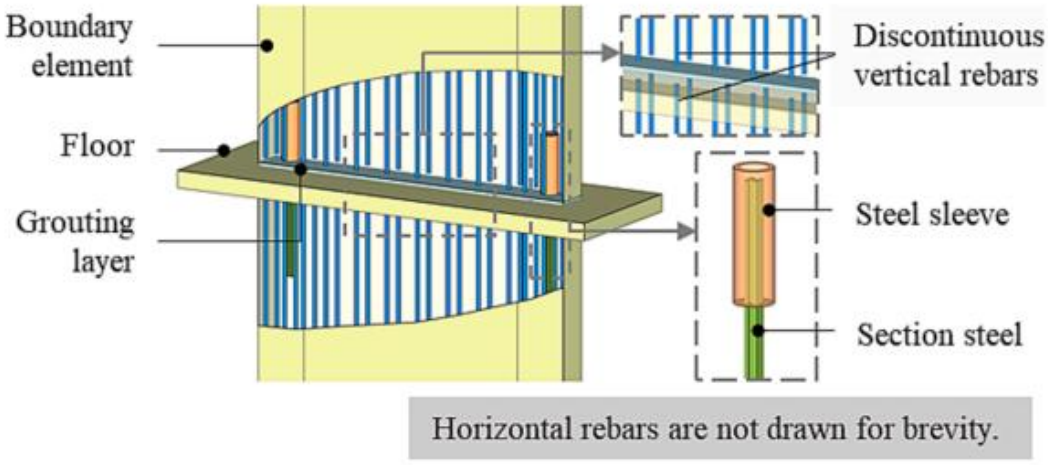

Figure 22 Sleeve grouting connection in precast concrete walls (Figure adapted from [34])

2. Spiral-confined lap connections

A recent connection solution for precast concrete shear walls (PCSWs) involves the use of spiral-confined lap splices, as illustrated in Figure 23. In this configuration, spiral reinforcement is arranged around the lapped dowel bars to provide additional confinement to the splicing region. This confinement enhances the bond performance between the lapped bars and the surrounding concrete, allowing for a reduction in the required lap length without compromising the structural integrity. Moreover, by shortening the lap length, this system facilitates faster on-site assembly of precast wall panels, contributing to improved construction efficiency and overall performance of the PCSW system [35].

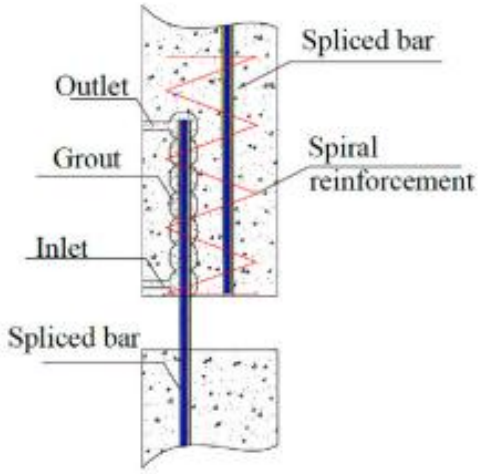

Figure 23 Spiral-confined lap splice (Figure adapted from [35])

Compared to grouted sleeve connections, which rely primarily on the bond provided by the grouting material, spiral-confined lap splices offer a more continuous and integrated reinforcement mechanism, potentially improving ductility and energy dissipation under seismic loading, while maintaining a simpler construction process [35].

3. Keyway connection

Keyway connections are commonly used in fabricated slab structures. The joints of prefabricated wall slabs are equipped with various keyways with uniform layout and regular keyways. The adjacent wall slabs are locked together by keyways, and concrete is poured during the occlusion. The prefabricated components are connected as a whole, and the size and arrangement density of the keyway have a great influence on the reliability of the connection.

In conclusion, this technology provides strength to the slab interfaces [21]. Figure 24 shows the union of the several prefabricated components that establish the beam-to-slab connection.

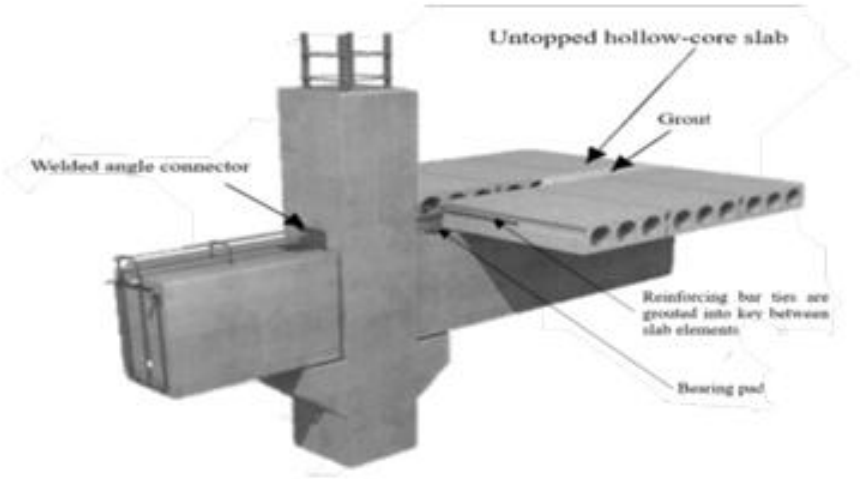

Figure 24 Slab to beam connection (Figure adapted from [21])

2.4 GAPS AND RESEARCH NEEDS

The literature review revealed that the growing evolution of the prefabrication sector allows fast and affordable construction, compared to traditional method, which is significantly useful in emergency situations. Based on this review, it was concluded that there is a need to construct structures more quickly, cheaply, lighter and with less environmental impact.

The dry connections, namely, bolted connections, appear to be a suitable solution to achieve these goals for low-rise buildings, while also enabling future deconstruction and reuse. Furthermore, improving the transmission of forces between walls is crucial to enhance the structural performance under extreme or accidental actions, such as severe earthquakes.

It is worth noting that studies investigating the seismic performance of precast concrete modular buildings using bolted connections are extremely limited. This scarcity of data highlights a significant gap in the literature and represents a

substantial avenue for further research, particularly in understanding the global structural behaviour, load transfer mechanisms, and the influence of connection detailing on modular precast systems.

This dissertation will add knowledge of the behaviour of modular precast buildings towards seismic occurrences. More specifically, the objective is to accurately model a building composed of insulated load-bearing walls connected through dry connections and assuming a rigid diaphragm, and subsequently to simulate its seismic response. In addition, the research includes a performance assessment of a full-scale building considering different seismicity levels, to evaluate the structural capacity and response across a range of earthquake intensities.

3 CASE STUDIES

3.1 INTRODUCTION

This Section describes first the proposed precast wall modular building system, with prototype buildings considered in previous studies (Section 3.2). Experimental results are available for connection sub-assemblies (Section 3.3) and these have also been modelled. Finally, for the purposes of this thesis, which relies on advanced nonlinear analysis as a tool for performance assessment, a smaller building has been devised for use during nonlinear modelling calibration, to be more manageable yet descriptive of all the system characteristics (Section 3.4).

3.2 PROPOSED PRECAST CONCRETE MODULAR WALL SYSTEM

The growing need for housing and the occurrence of extreme events have increased the need to develop new faster construction solutions, with controlled costs. In addition, there is a concern for more durable and sustainable solutions. Precast concrete structures have been widely used because its many advantages, such as, high quality, high industrialization, low workmanship and high durability, compared to traditional on-site construction. The aim of "R2UTechnologies Modular Systems" project is to take advantage of the excellent concrete properties, maximize the benefits of prefabrication and improve the sustainability of structures, by decreasing the carbon embodied in concrete structures, as well as increasing their durability [14].

3.2.1 Wall panels

In this study, we focus on the modular wall system developed by the innovative *"R2UTechnologies Modular Systems"* project, which introduces an insulated load-

bearing composite wall with a structural function for buildings. The wall consists of two concrete layers separated by a non-structural core material, which provides thermal and acoustic insulation. At the extremities of the panel, however, the wall is composed of a single solid concrete layer to ensure structural continuity and load transfer, which represents the main difference compared to sandwich panels (Figure 25).

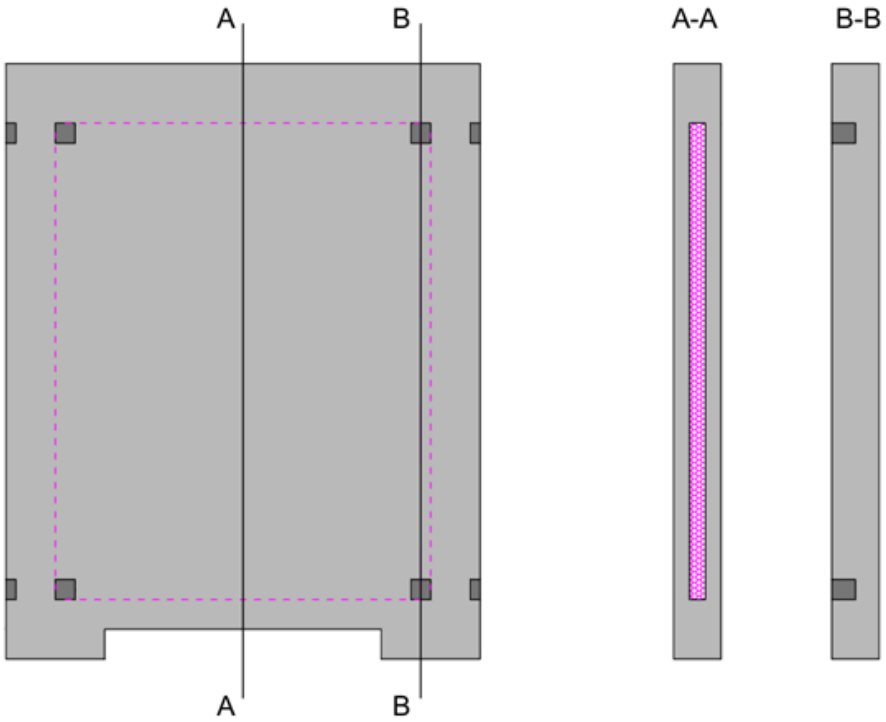

Figure 25 Load-bearing insulated wall (Figure adapted from [36])

The entire wall is prefabricated in the factory, ensuring higher quality control and minimizing the risk of inadequate detailing during on-site assembly.

These panels can be designed to sustain the dead loads of the building elements placed above them. Such load-bearing panels require additional strength to withstand various load conditions, which has led to the development of specific design approaches and testing methods. In this case, the vertical loads are transferred directly to the foundation, as illustrated in Figure 27 [18].

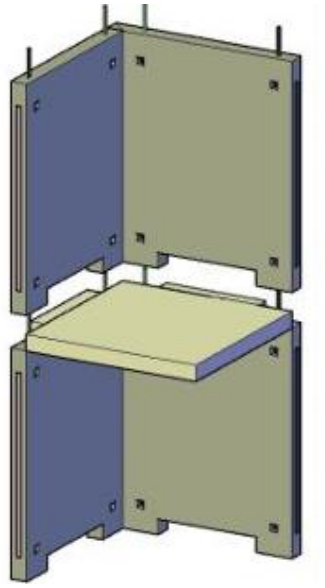

Figure 26 Load-bearing wall resisting system with dry connections for residential buildings (Figure from [36])

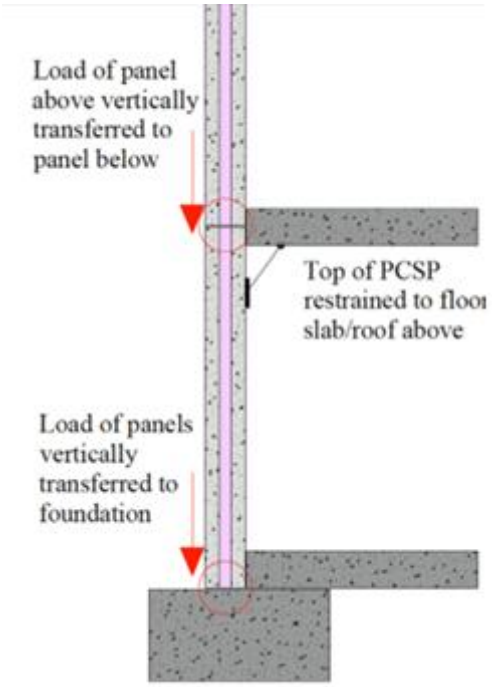

Figure 27 Load bearing carrying panels above only (Adapted from Figure from [18])

3.2.2 Floor slabs

Floor systems in buildings primarily serve the function of transferring vertical loads to the vertical load-resisting structural elements. In addition, precast floors

often play a fundamental role in the overall stability of the structure, as they can transmit horizontal loads through diaphragm action towards the stabilising units. Among the various types of precast floors, this study focuses on hollow-core slabs, which represent one of the most widely adopted solutions in modern precast construction.

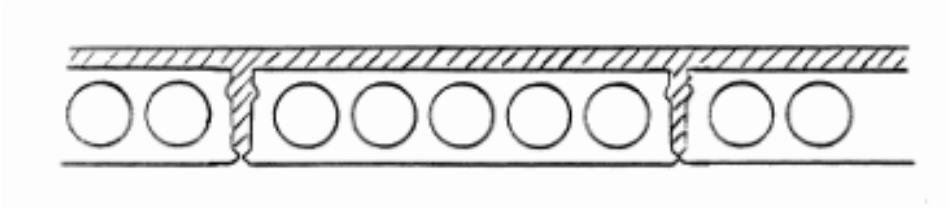

Figure 28 Hollow-core floors (Figure adapted from [2])

Prestressed hollow-core units are characterized by longitudinal voids or cores, whose purpose is to optimise material usage while reducing the overall weight of the slab. As illustrated in Figure 28, these units typically measure 1200 mm in width and can reach lengths of up to 20 m. The edges are profiled or keyed to ensure proper vertical shear transfer across the grouted joints between adjacent units, thereby guaranteeing structural continuity and performance [19].

3.2.3 Connections

Prefabricated walls are interconnected with each other and with other structural components through vertical and horizontal connections. The main challenge was to ensure proper compatibility in terms of both stiffness and strength, while meeting the required tolerances for assembly, essential for adequate structural performance.

The walls are connected vertically at both ends using anchor bolts, creating a dry connection that facilitates demountability and reuse, thereby enhancing the lifecycle performance of the system. The vertical connection consists of steel bars

with a total length of 600 mm and a diameter of 25 mm, as illustrated in Figure 29. Experimental tests on these connections were carried out, and their setup are described in Section 3.3, and the results are described in detail in Section 5 [37].

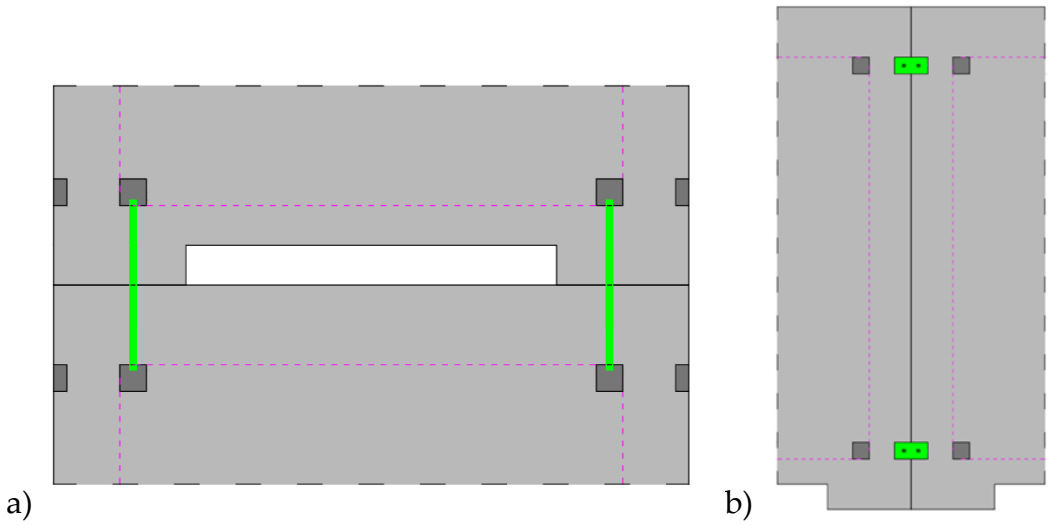

Figure 29 Proposed structural system: a) wall to wall vertical connection; b) wall to wall horizontal connection.

For the horizontal connections between panels, three innovative dry-bolted connection systems were developed. All proposed solutions employ anchored steel plates and high-strength bolts to ensure efficient stress transfer between the connection and the precast wall. For this purpose, rebars anchored to the inner concrete layer and welded to the steel plate were adopted, as this anchorage system provides a large contact surface between steel and concrete, thereby enhancing the bond strength. Moreover, the steel plates were designed with oval-shaped holes oriented in different directions to accommodate the tolerances required during on-site assembly [38].

The Connection-1 is shown in Figure 30 and is not symmetrical, one side has the steel plate inserted into the wall, with an opening for the bolt installation, while on the other side, the steel plate is outside the wall.

a) 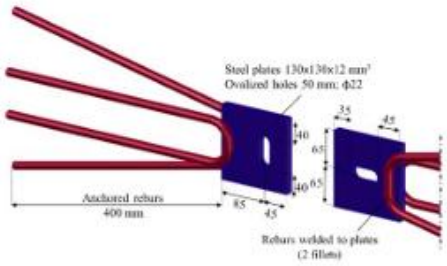

b) 

Figure 30 Configuration of Connection-1: a) (Figure adapted from [38])

Connection-2, shown in Figure 31, is symmetrical, with a variation in the ovalized hole orientation. The plates are arranged perpendicular to the wall, with an opening for tightening the bolt.

a) 
b) 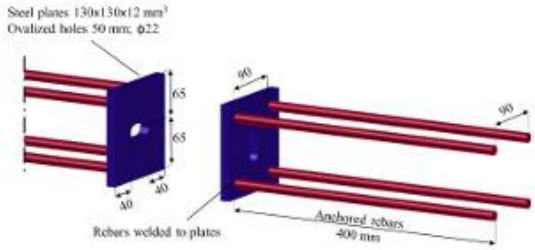

Figure 31 Configuration of Connection-2: a) (Figure adapted from [38])

In Connection-3 (Figure 32) the bolts are already welded to the plate, and an extra plate is used to connect both sides, with two ovalized holes.

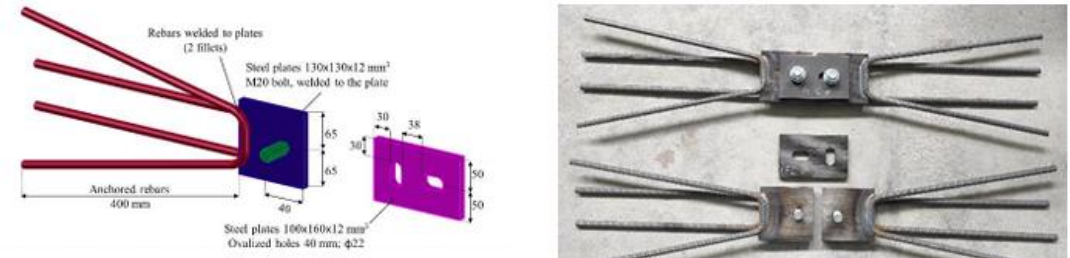

a) b)

Figure 32 Configuration of Connection-3: a) (Figure adapted from [38])

In the present study, the focus is on the modelling of the first type of connection proposed.

3.3 CONNECTION SUBASSEMBLIES

In this section, the specimens tested on the wall-to-wall vertical connections are described.

An experimental program was carried out involving a total of seven connection typologies for horizontal joints, with the aim of investigating the influence of: i) the extension of the solid concrete at the top end of the wall; ii) the arrangement of reinforcing bars (both horizontal and vertical) around the opening where the steel bolt is positioned; and iii) the cyclic loading conditions. To achieve this, a simplified approach was adopted by analysing a single connection, which allowed a more detailed characterization of the effects of the studied parameters. For this purpose, a representative wall specimen (see Figure 33(a)) with only one connection was constructed, and a common geometry was maintained across all groups (Figure 33(b)) [36].

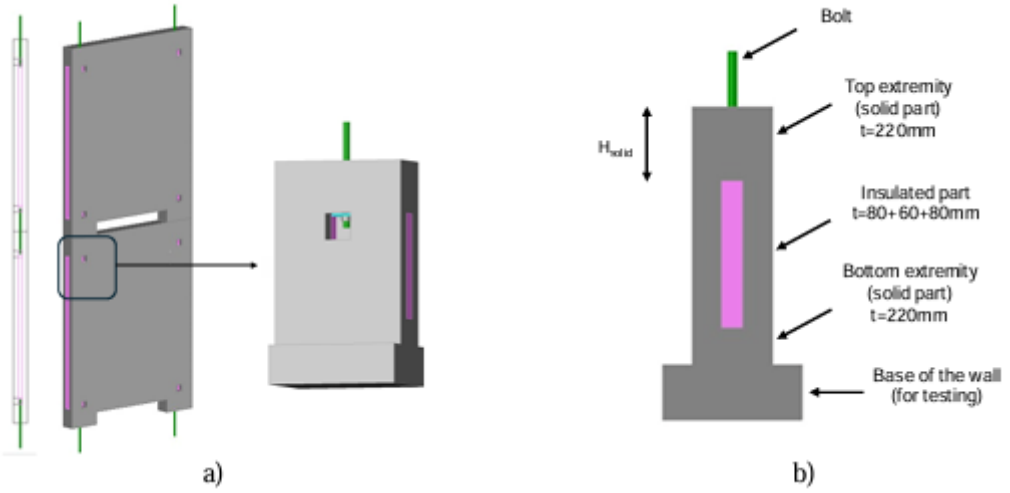

Figure 33 Load-bearing walls with bolted connections: (a) Representative single-connection specimen of the proposed structural system; (b) Profile view of the single connection specimen, highlighting common characteristics. (Figure from [36])

Four groups (2, 3, 4, and 6) were considered, each consisting of three specimens, whose details are shown in Figure 34.

Each specimen has a total height of 0.50 m, a width of 0.70 m, and a thickness of 0.22 m. Additionally, each specimen includes a foundation part with a thickness of 0.40 m, designed to secure the wall in place during testing. All walls were reinforced with a ϕ5/200 mm mesh near both faces of the wall. The main variations between the four groups are: i) Different lengths of the solid concrete zone at the top extremity (100 mm or 200 mm); and ii) Variations in the relative positioning of the vertical and horizontal reinforcement bars (type 1 and type 2 reinforcing rebars, respectively) [36].

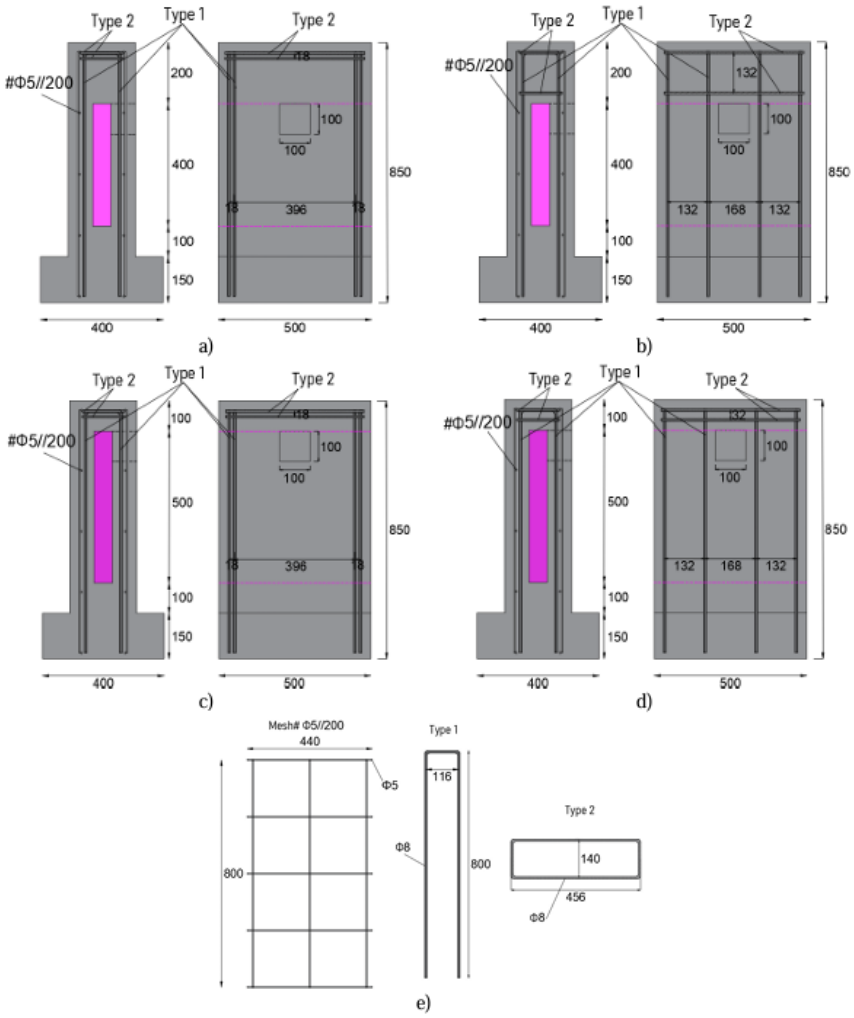

Figure 34 Geometry and reinforcement detailing of the specimens: a) Group 2, b) Group 3, c) Group 4, d) Group 6, and e) mesh and type 1 and 2 rebars configuration. (Figure adapted from [36])

In each group, the first test consisted of a monotonic tensile strength test carried out under displacement control at a rate of 0.01 mm/s. From the corresponding force–displacement curve, the yield displacement (dy) was determined and subsequently adopted to define the loading protocol for the cyclic test. The second test in each group was a cyclic tensile test, until failure occurred. Finally, the third test was another monotonic tensile test, executed under the same displacement control conditions as the first one [36].

In Chapter 5, each specimen was modelled in SAP2000 to validate the experimental force–displacement curves derived from the tests.

3.4 SMALL BUILDING FOR NONLINEAR ANALYSIS CALIBRATION

This section focuses on the presentation of the simplified small building, including a detailed description of the geometry, structural system, materials, and applied loads.

This configuration was adopted for the nonlinear analysis's calibration. Specifically, two models were considered: a two-dimensional model and a simplified three-dimensional model consisting of two walls connected by slabs.

3.4.1 Geometrical Description

The small building model consists of four floors, as descripted in Figure 35, with a total height of 12 metres each level has a height of 3.00 metres. Standardised panels were adopted, with lengths of 2.40 metres and 4.80 meter, and a thickness of 0.20 metres consisting of two 8 cm concrete layers enclosing a 4 cm insulation layer.

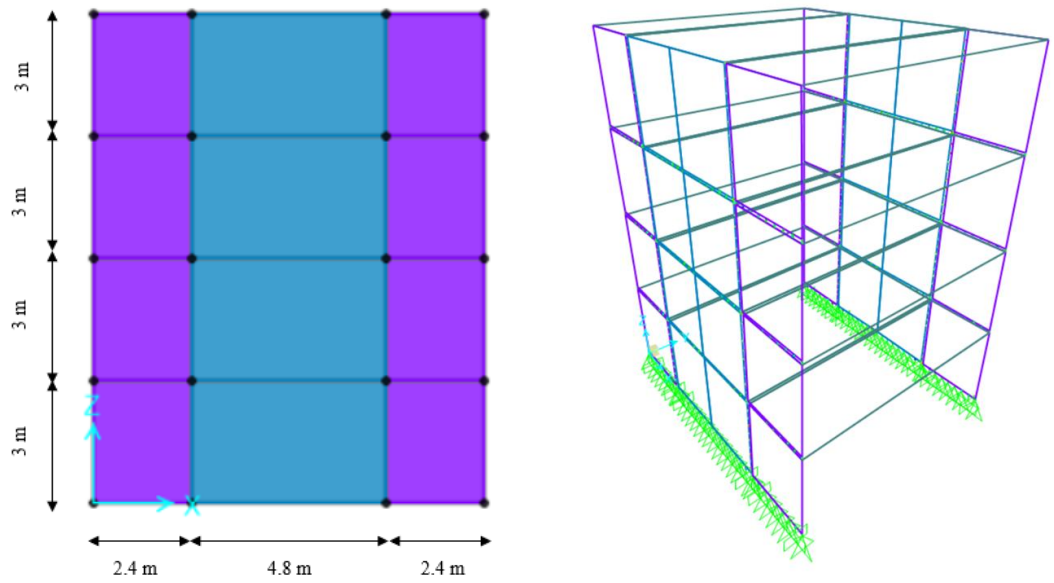

Figure 35 View of small building model

Additionally, in the three-dimensional model, the floor system was represented by hollow-core slabs 0.16 m thick, topped with a 0.07 m reinforced concrete layer.

a) 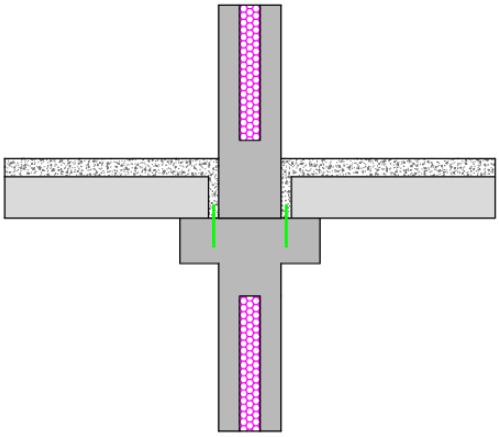 b) 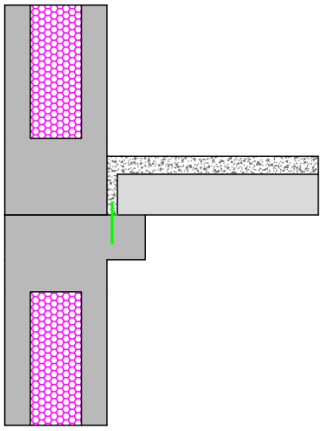 .

Figure 36 Cross-section: a) Internal wall; b) Perimetral wall

All connections are standardised joints and special joints as mentioned in Section 4.2.

3.4.2 Material and Loads

The concrete adopted for this structure was C50/60 class and its characteristics were obtained from the Eurocode 2:

Concrete C50/60	
f_{ck}	50 MPa
$f_{ck,c}$	60 MPa
f_{cm}	58 MPa
f_{ctm}	4.1 MPa
E_{cm}	37 GPa
ϱ_c	25 kN/m3
υ	0.2

Table 1 Characteristics of the concrete C50/60 class

- E_{cm} is the Young's modulus of the concrete
- ϱ_c is the density of concrete

- υ is Poisson's ratio of concrete
- fck is the Characteristic compressive cylinder strength of concrete at 28 days
- fck,c is the Characteristic compressive cube strength of concrete at 28 days
- fcm is the Mean compressive strength
- $fctm$ is the Mean value of axial tensile strength of the concrete

The steel used was B450 C grade steel for the reinforcement and connecting bars and its characteristics were attained from the Eurocode 2:

Steel B450C	
f_{yk}	500 MPa
f_{ym}	550 MPa
E_s	200 GPa
ϱ_s	77 kN/m3
υ	0.3

Table 2 Characteristics of the steel B450C

- E_s is the Young's modulus of the steel
- f_{yk} is the Characteristic yielding force
- f_{ym} is the Mean yielding force
- ϱ_s is the Density of the steel
- υ is the Poisson's ratio of steel

The next phase consists of defining the load combinations, particularly the definition of the floor load. This load was set as 9.5 kN/m^2 and results of the design seismic action with the self-weight (4.5 kN/m^2), permanent loads (3 kN/m^2) and imposed loads on the horizontal elements (2 kN/m^2). The self-weights of the walls were explicitly accounted for by the calculation software.

4 NUMERICAL MODELLING

Numerical modelling was performed using SAP2000, a software specifically developed for structural analysis for the purpose of design, assessment and retrofitting. It enables the analysis of seismic behaviour in various structures, under equivalent static loads or full dynamic excitation, while accounting for material inelasticity and geometric non-linearities.

4.1 PRECAST CONCRETE WALLS MODELLING

The proposed wall is composed by two layers of concrete, 80 mm thickness and a layer of insulation, 40 mm thickness for a total width of 200 mm. Both concrete layers were reinforced with a B450C steel bars mesh Φ8/100 mm.

Several modelling options were considered for the panels, ranging from the simplest approach, elastic shell elements, to more refined representations, including layered sections with uncoupled (directional) and then coupled materials. A detailed comparison of the results obtained from these different approaches is presented in Section 6. Based on this comparison, the most appropriate modelling strategy for the panels was to represent them using shell layered sections with equivalent thicknesses, as shown in Table 3.

						Material Component Behavior			
Layer Name	Distance	Thickness	Type	Material	Material Angle	Type	S11	S22	S12
1	0.06	0.08	Shell	C50/60	0	Coupled	Nonlinear	Nonlinear	Nonlinear
2	0.06	0.0005	Shell	B450C	0	Directional	Nonlinear	Inactive	Inactive
3	0.06	0.0005	Shell	B450C	90	Directional	Nonlinear	Inactive	Inactive
4	0	0.04	Shell	insulation	0	Directional	Linear	Linear	Linear
5	-0.06	0.0005	Shell	B450C	0	Directional	Nonlinear	Inactive	Inactive
6	-0.06	0.0005	Shell	B450C	90	Directional	Nonlinear	Inactive	Inactive
7	-0.06	0.08	Shell	C50/60	0	Coupled	Nonlinear	Nonlinear	Nonlinear

Table 3 Shell Layered

The coupled material model suggested by Darwin Pecknold [39] was proposed for the concrete and it is represented in the Figure 37 .

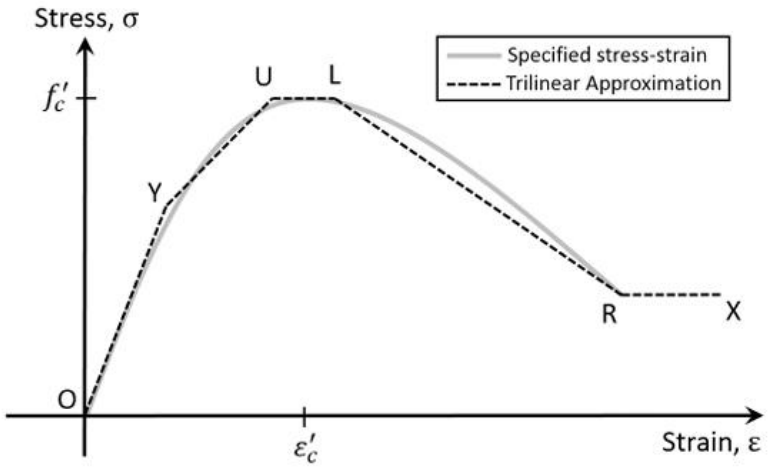

Figure 37 Stress-strain model of concrete proposed by Darwin Pecknold (Figure from [39])

This model represents the concrete compression, cracking, and shear behaviour under both monotonic and cyclic loading. The direction of cracking can change during the loading history, and the shear strength is affected by the tension strain in the material. The axial stress-strain curve specified for the material is simplified to account for initial stiffness, yielding, ultimate plateau, and strength loss due to crushing. Compressive strength reduction based on perpendicular tensile strain is accounted for as described in Vecchio and Collins (1986) [40].

Vecchio and Collins showed that the compression strength of concrete depends on the magnitude of the tensile strain in the perpendicular direction. The effective compression strength of concrete in such situations can be substantially smaller than the original f'c.

The following equation is used for the compression strength reduction factor, r:

$$r = \frac{1}{0.8 - 0.34\frac{\varepsilon m}{\varepsilon_c'}} \leq 1 \quad (1)$$

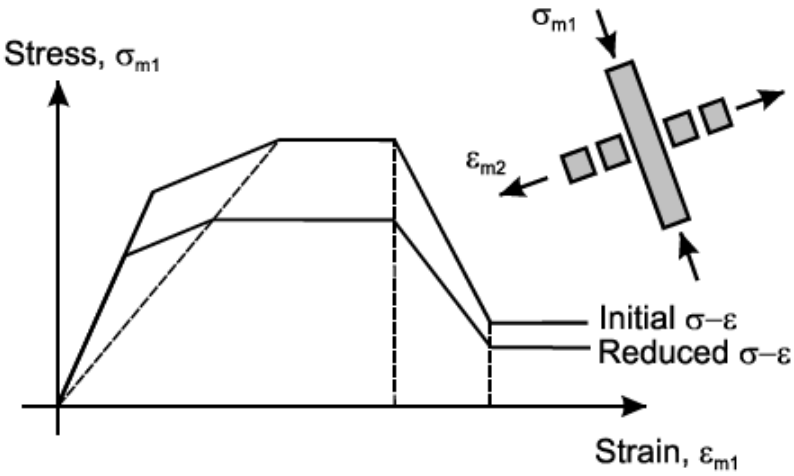

Figure 38 Change in Stress-Strain Relationship to Account for strength reduction (Figure from [39])

This approach allows for a more realistic representation of the structural response, especially under conditions where cracking, crushing, or other inelastic behaviours may occur.

4.2 CONNECTIONS MODELLING

Prefabricated walls are connected to each other and to other structural elements using vertical and horizontal connections.

The panels are placed on top of each other and are connected vertically by reinforcement bars and horizontally by bolted dry connections, basically the horizontal interface consists of concrete-to-concrete contact and reinforcement bars, and the vertical interface consists of bolt connections and gap elements.

4.2.1 Horizontal Interface: Reinforcement Bars

In the model the bars are represented by a *Plastic (Wen)* nonlinear link, consisting of a horizontal and vertical stiffness. The directions are assumed to be uncoupled, hence the characteristics for each direction can be determined independently.

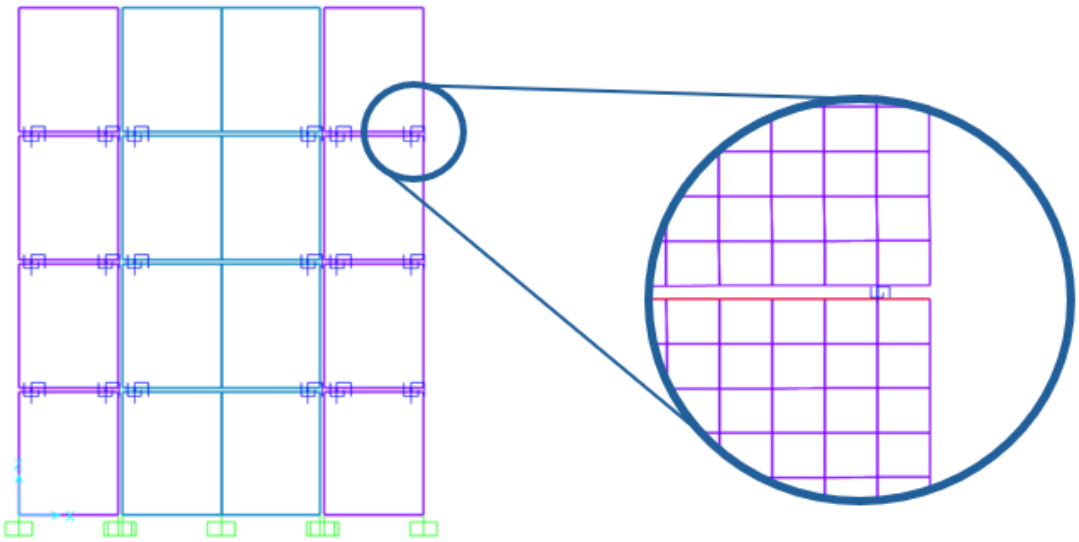

Figure 39 Reinforcement bars located at the horizontal interface

A large amount of research has been conducted to study the bond behaviour of reinforcement in concrete. In pull-out testes, a force is applied to a reinforcement bar embedded in concrete. During the test different parameters are monitored. From these parameters several relationships have been obtained.

For the modelling of the axial direction the behaviour is simplified and idealised as bilinear. Three parameters describe the bilinear spring: elastic stiffness K1, yield force Fy and the post-elastic stiffness ratio.

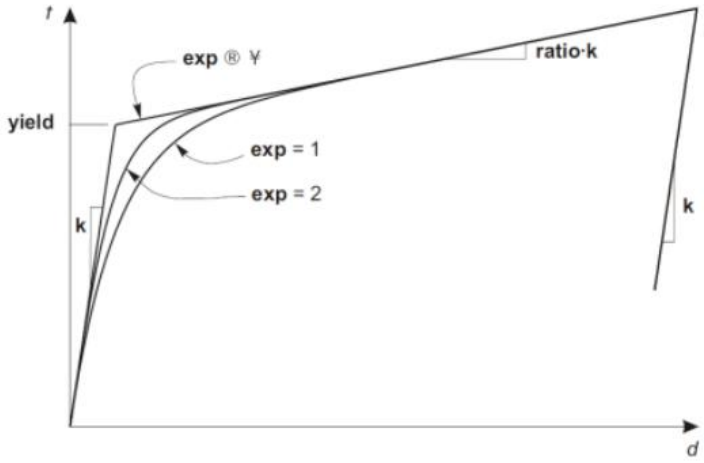

Figure 40 Bilinear behaviour (Plastic Wen)

The initial elastic stiffness of the axial spring, modelled as a simple free steel bar under tension/compression was determined using the classical expression for a free bar:

$$k_1 = \frac{E_s \cdot A_s}{l} \tag{2}$$

In this case, the steel bar has a total length of 600 mm, with 300 mm embedded in the top panel and 300 mm in the bottom panel.

To determine the yield force, it was assumed, that all failure mechanisms other than yielding are prevented. Hence the yield force is given by:

$$F_y = A_s * f_s \tag{3}$$

In the numerical model, however, the ultimate force (*Fu*) was directly introduced instead of the yield force (*Fy*), with a post-yield stiffness ratio set to zero and a yielding exponent of 10.

As for the axial direction, for modelling the lateral direction (dowel action) behaviour is simplified and idealised as bilinear with a Plastic Wen link (Figure

40). Three parameters describe the bilinear spring: elastic stiffness K1, yield force Fy and the post-elastic stiffness ratio.

The displacement response due to lateral force of the reinforcement bar is influenced by the aspects such as the joint width, the bar diameter, the quality of concrete and steel.

Among the many proposals of models to represent the so-called dowel action the one proposed by Tsoukantas and Tassios (1989) [41] is adopted in the following. The corresponding force-displacement curve is shown in Figure 41.

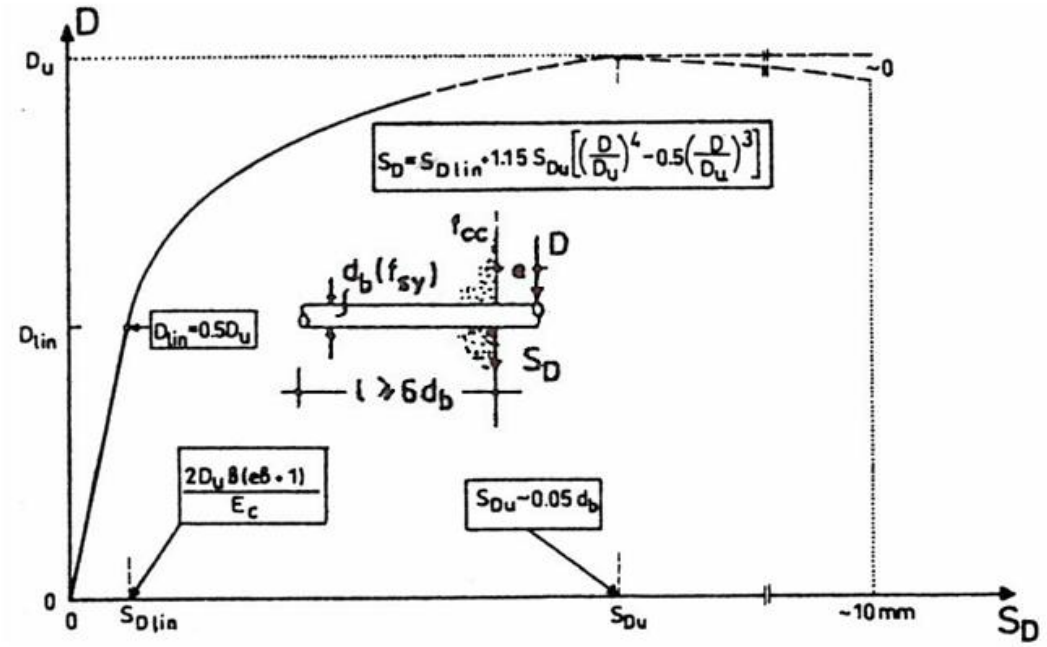

Figure 41 Force-displacement curve predicted by S.G. Tsoukantas and T.P. Tassios (Figure from [41])

The initial stiffness is given, according to Tsoukantas and Tassios by:

$$k_1 = \frac{F}{D} = \frac{E_c}{4 \cdot (\beta(e\beta + 1))} \rightarrow e\beta^2 \cong 0 \rightarrow k_1 = \frac{E_c}{4\beta} \tag{4}$$

Where:

$$\beta = \left(\frac{E_c}{8 \cdot E_s \cdot I_s}\right)^{1/4} \quad (5)$$

So, we can rewrite the previous equation as:

$$I_s = \frac{64 \cdot d^4}{\pi} \rightarrow k_1 = \left(\frac{2 * E_c^3 * E_s}{\pi}\right)^{1/4} * d \quad (6)$$

That equation shows that the lateral stiffness K1 is linearly dependent on the diameter of the bar, and the deformability of the surrounding concrete (Ec) is more influential than that of the steel bar.

The limiting force for which the response remains in the elastic stage is given, according to Tsoukantas and Tassios by:

$$F_{lim} = 0.5 * d^2 * \delta * \sqrt{f_s * f_{ck}} \quad (7)$$

Where δ is a factor (<1.3) depending on the available concrete cover of the bar in the direction of the shear force. In this study, since no perfect contact between the connection and the surrounding concrete is ensured in the initial phase, the factor δ was set equal to 1.

Also in this case, a post-yield stiffness ratio equal to zero was adopted, and the ultimate strength was defined according to Tsoukantas and Tassios as twice the limiting force.

4.2.2 Horizontal Interface: Friction element

The concrete-to-concrete interface is represented by the contact between adjacent panels. When compressive forces act on the interface, shear resistance is mobilized primarily through friction.

From the limited test results available in the literature on the shear capacity of precast concrete wall connections, a wide scatter of the friction coefficient is observed, with values ranging from 0.2 to 1.59. In the work of Tsoukantas and Tassios (1989) [41] more specific additional information is provided from which a realistic lower-bound value for the friction coefficient, across both smooth and rough surfaces, has been obtained.

Since the precast panel surfaces are generally smooth, the value for smooth interfaces has been used for the friction coefficient.

$$\tau_{fr,u} = 0.4 \cdot \sigma_{cc} \tag{8}$$

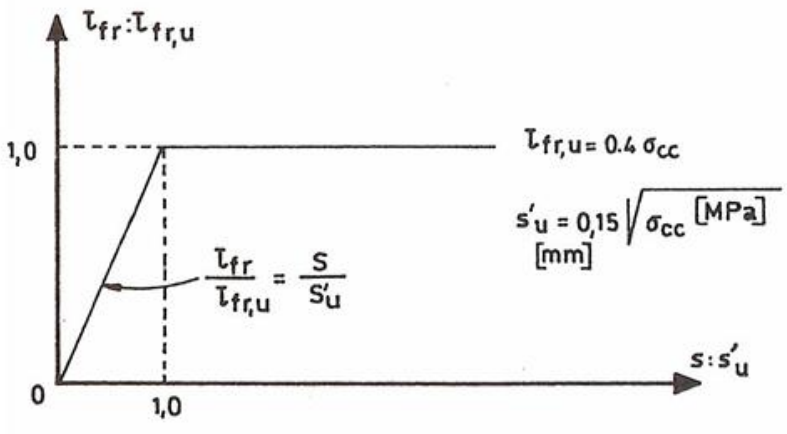

Figure 42 Friction-shear stress versus shear displacement curve

To model the frictional behaviour of the interface the *Friction Isolator* element implemented in the employed program has been used. The available element

works as a gap-element (no tension) with a compression-branch consisting of an elastic spring in series with a friction device.

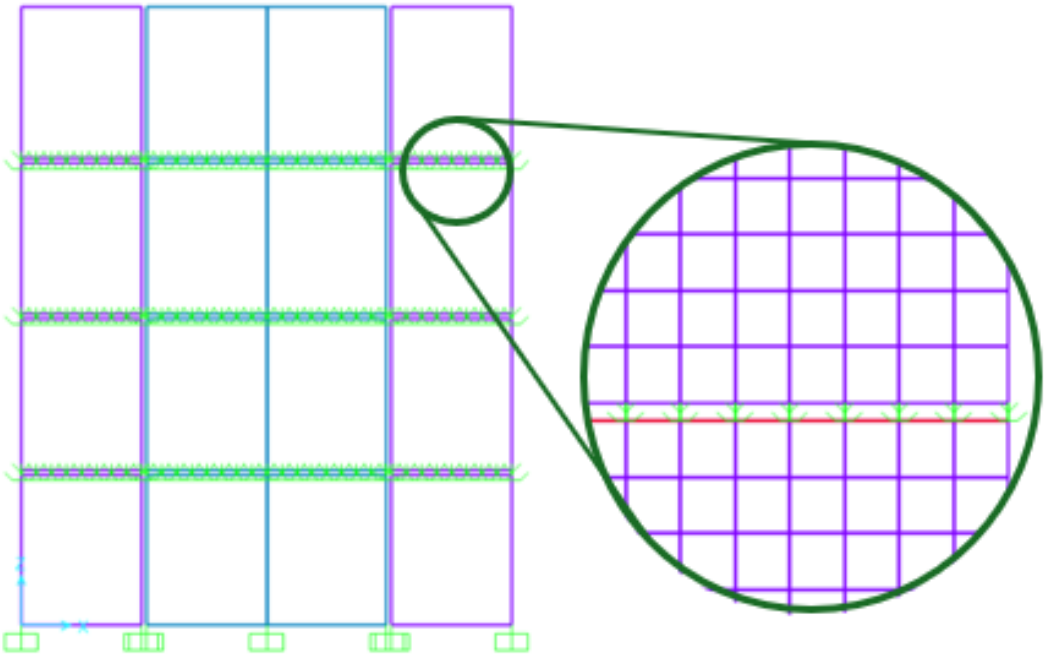

Figure 43 Friction element located at the horizontal interfaces

In order to define this element, both the stiffness and the friction coefficient must be specified. The stiffness was determined following the formulation proposed by Tsoukantas and Tassios, by averaging the normal forces acting on the interface surface.

$$k = \frac{\tau_{fr,u}}{s'_u} = 2.67 \cdot \sqrt{\sigma_{cc}} \tag{9}$$

The radius of this element was set to a very large value (= 100) to represent a flat sliding surface.

4.2.3 Vertical Interface: Bolt Connections

Under lateral load the connections along the vertical interface have to ensure the transmission of the shear action. In addition, the connections transfer the lateral pressure between adjacent panels.

In the considered wall system, the only vertical connections are located at the vertical interface, with two connections provided per panel.

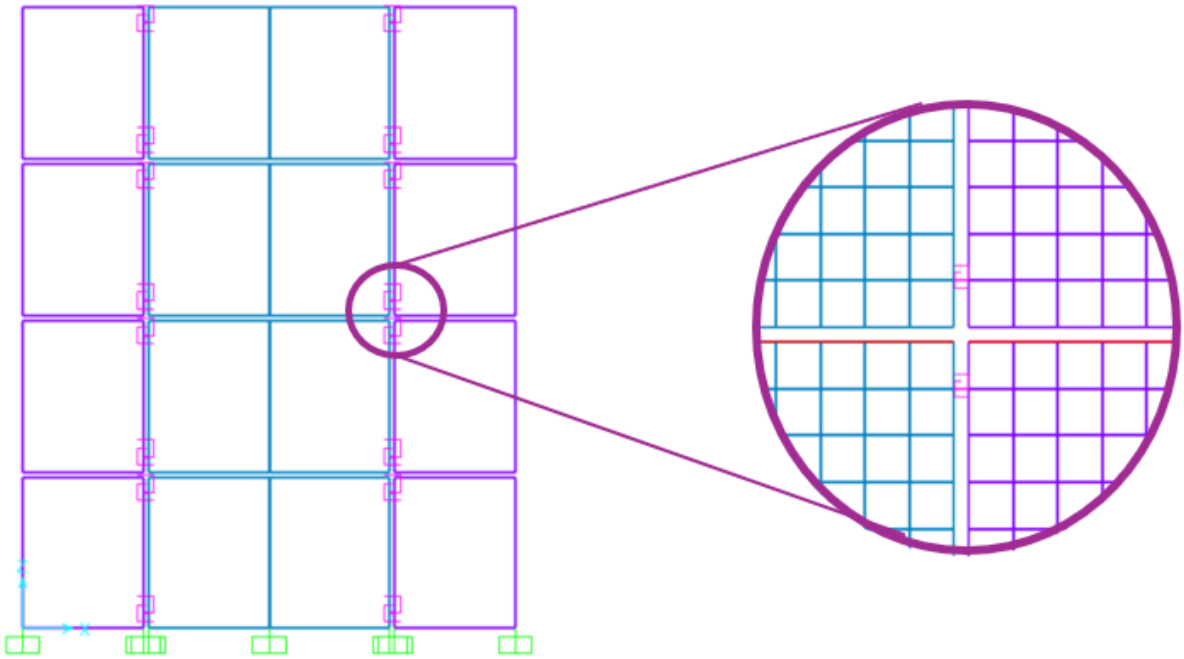

Figure 44 Bolt connections located at the vertical interfaces

There are three proposed demountable connections consist of anchored steel plates and high-strength bolts (Section 3.2.3). This type of anchorage has been chosen because it provides a high contact surface between the concrete and the steel, the steel plates were designed with ovalized holes in perpendicular directions to comply with the tolerances required during the on-site assemblage.

The proposed connections were designed following the Eurocode 3 recommendations.

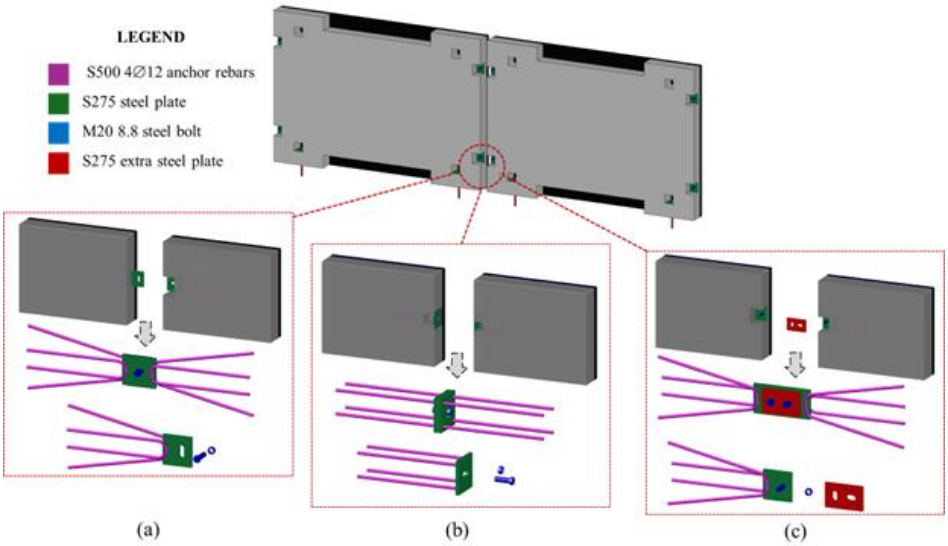

Figure 45 Configuration of vertical Connections

To model these connections the *Multilinear Plastic Link* elements were employed. Their calibration was calibrated using the behaviours obtained from monotonic shear and tensile tests.

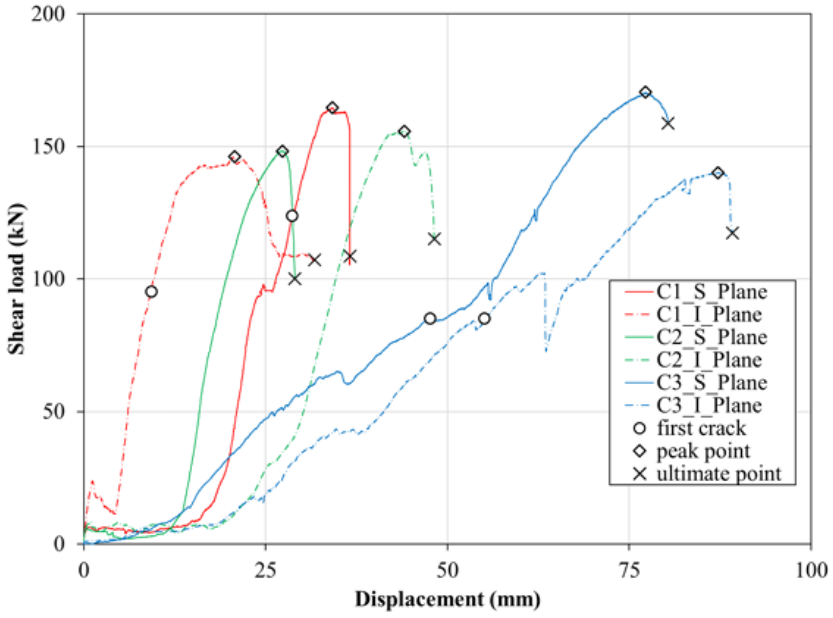

Figure 46 In-plane shear load-displacement curves (Figure from [38])

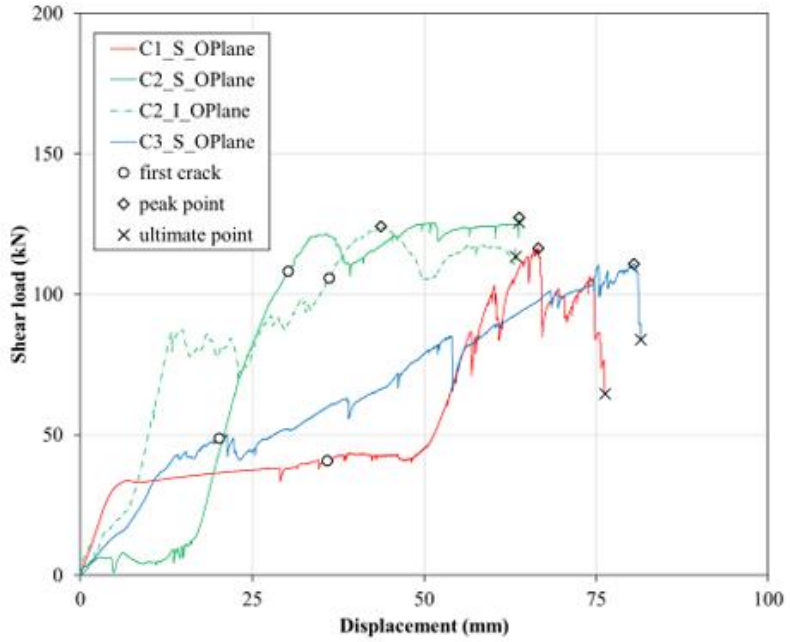

Figure 47 Out-of-plane shear load-displacement curves (Figure from [38])

This modelling strategy was adopted to achieve a more representative simulation of the actual structural behaviour, explicitly accounting for the initial slack observed in the connections, which delays their activation.

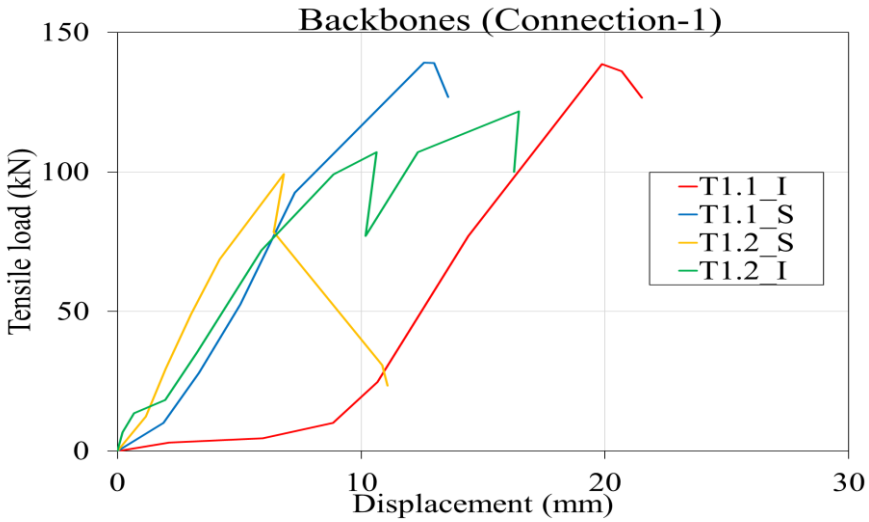

Figure 48 Tensile load-displacement curve (Connection-1)

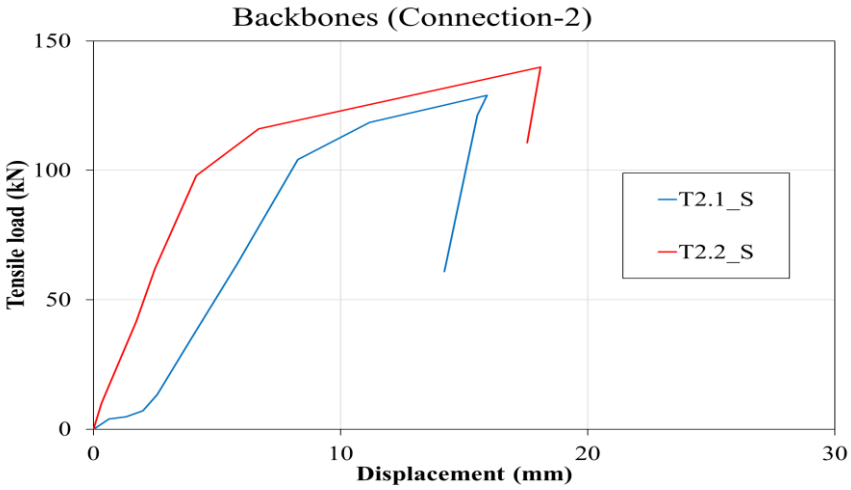

Figure 49 Tensile load-displacement curve (Connection-2)

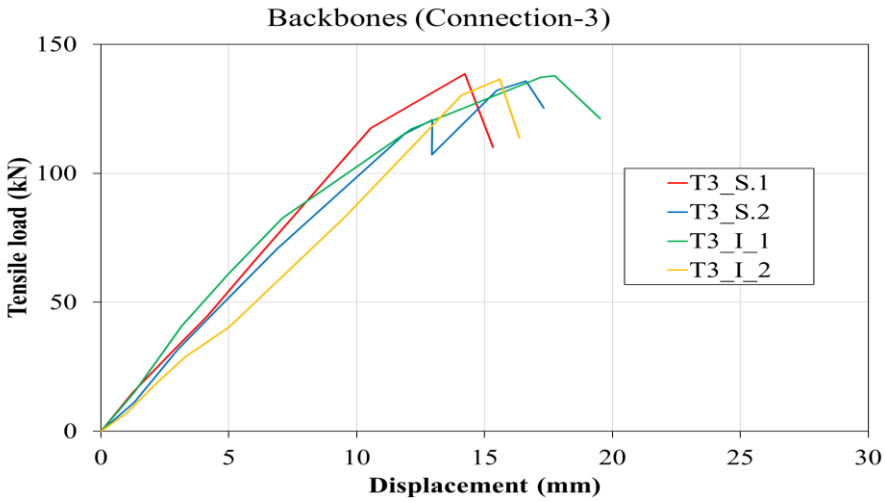

Figure 50 Tensile load-displacement curve (Connection-3)

The specimens were identified according to the following rules: the type of connection (1, 2 or 3); the roughness of the steel plate (smooth, "S" or indented, "I") and load application (in-plane, "Plane", or out-of-plane, "OPlane").

The out-of-plane behaviour (Figure 47) was explicitly defined only in the full building model, as it was not required in the simplified configurations.

4.2.4 Vertical Interface: Gap element

For the vertical interfaces, multilinear link elements are adopted to model the bolted connectors, while simple *Gap elements* are introduced to prevent overlapping between panels. These gap elements can only transmit compression forces. In the vertical direction, their spring stiffness is set to zero, since the panels are physically separated and the normal contact forces are negligible.

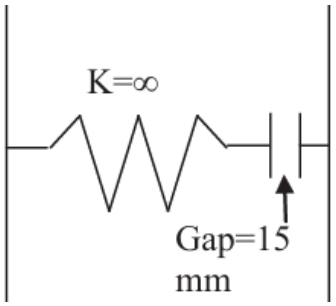

Figure 51 Schematisation of the Gap element

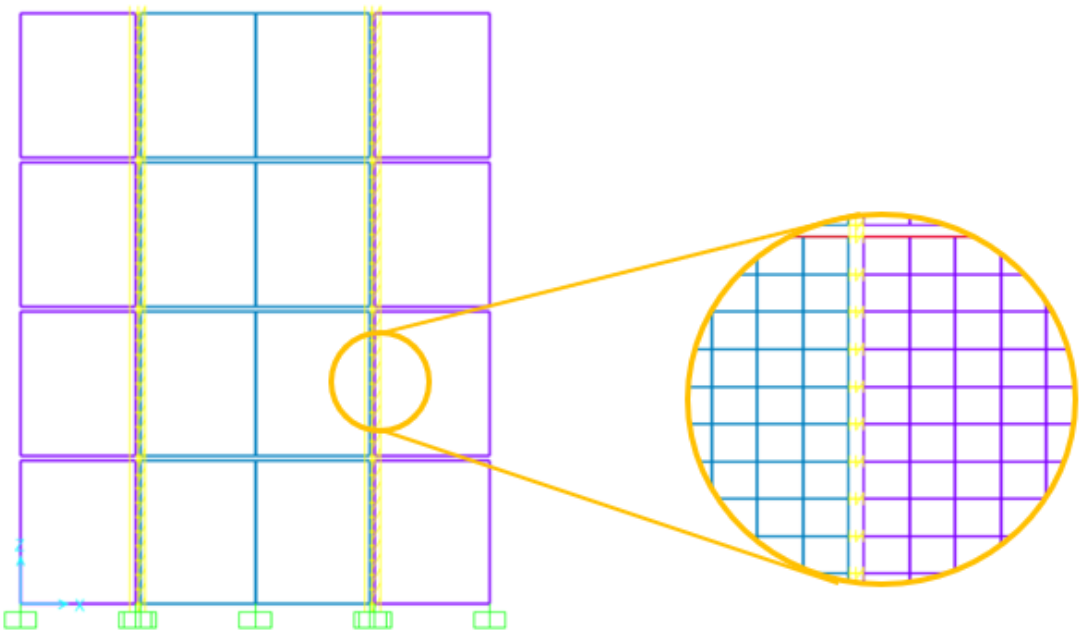

Figure 52 Gap elements located at vertical interfaces

4.3 SLABS MODELLING

About the floors, the system considered consists of prestressed hollow-core precast units with a thickness of 16 cm, topped with a 7 cm layer of reinforced concrete. The hollow-core units, 1200 mm wide, feature profiled edges to ensure adequate vertical shear transfer, while the reinforced concrete topping provides continuity and stiffness, enabling the floor to act as an effective horizontal diaphragm. This diaphragm action is crucial in seismic regions, as it allows the floors to distribute lateral forces to vertical resisting elements, thereby contributing to the overall structural stability under earthquake loading.

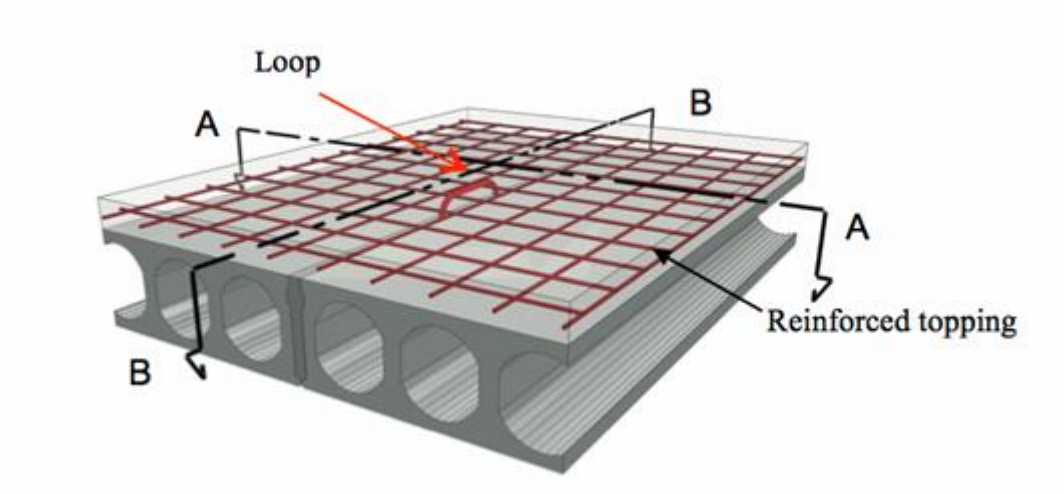

Figure 53 Hollow-core units (Figure from [19])

Several modelling approaches were considered for the floor to determine the most representative configuration (Figure 54):

1. Single continuous shell (thickness: 23 cm)
2. Single shell thickness: 7cm (top layer only)
3. Frame hinged at the extremities (1.2m x 0.16m) + single shell thickness: 7cm
4. Alternating shell not intersecting the vertical joint (thickness: 23 cm)

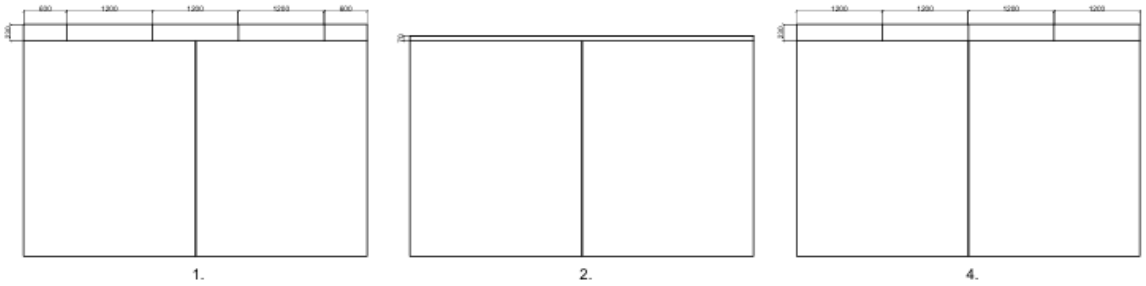

Figure 54 Different types of modelling slabs

Based on the shear verifications, the slab was idealized as a single shell element with an equivalent thickness of 15 cm, corresponding to the shear-effective depth.

$$h_{shear} = 7cm + \frac{16cm}{2} = 15cm \tag{10}$$

The subsequent section reports the verifications performed.

4.3.1 Shear Capacity Verification

We considered elastic floors, and the shear verification was carried out for the following cases: (i) a single continuous shell with a thickness of 23 cm, and (ii) a single shell with a thickness of 7 cm.

The verifications were performed both in accordance with the provisions of Eurocode 2 and using the reference values provided in the catalogue of prefabricated floor systems (Vigobloco).

According to Eurocode 2 (EN 1992-1-1 §6.2), the design shear resistance of a member without shear reinforcement is:

$$V_{Rd,c} = \left[C_{Rd,c} k (100 \rho_l f_{ck})^{1/3} + k_1 \sigma_{cp}\right] b_w d \tag{11}$$

Where:

$$C_{Rd,c} = \frac{0.18}{\gamma_c} \tag{12}$$

$$k = 1 + \sqrt{200/d} = 2 \tag{13}$$

$$\rho_l = \frac{A_{sl}}{b_w d} \tag{14}$$

For this case study, the effect of post-tensioning was neglected; consequently, the contribution of the $k_1\sigma_{cp}$ term was set equal to zero.

To verify that the applied shear does not exceed the design shear resistance, as prescribed by Eurocode 2, the following condition was checked:

$$V_{Ed} \leq V_{Rd,c} \tag{15}$$

In this study, V_{Ed} was taken as the average of the shear forces obtained from a nonlinear static (pushover) analysis. This approach was adopted because shear stresses tend to concentrate at the gaps between the panels, and the local maximum may overestimate the overall demand. By considering the average shear in the region of interest, a representative value of the applied shear was obtained for comparison with the design shear resistance.

Results for all the considered cases are illustrated in the following figures.

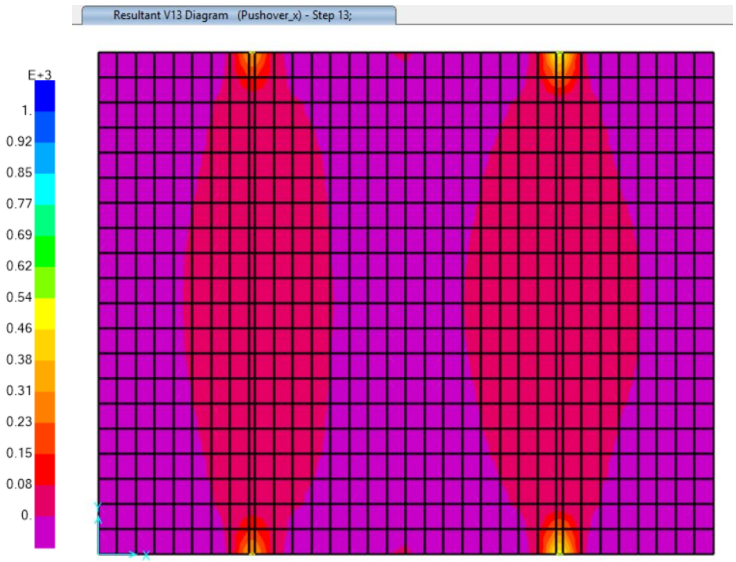

Figure 55 Shear V13: model with 23 cm thick slab

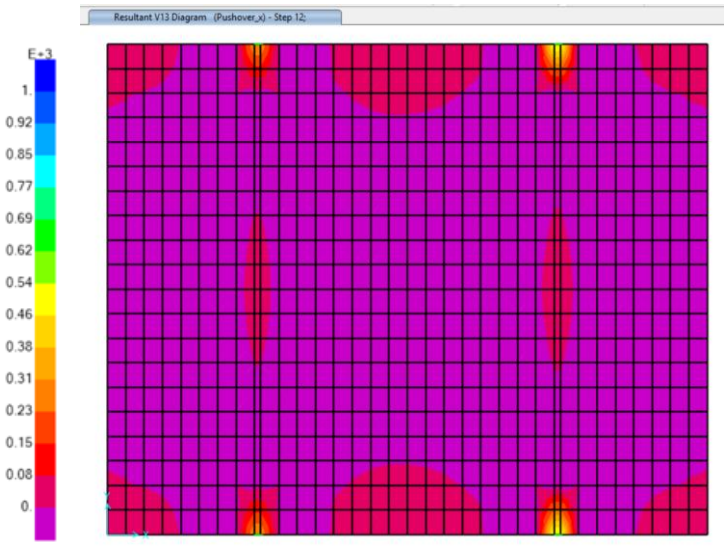

Figure 56 Shear V13: model with 7 cm thick slab

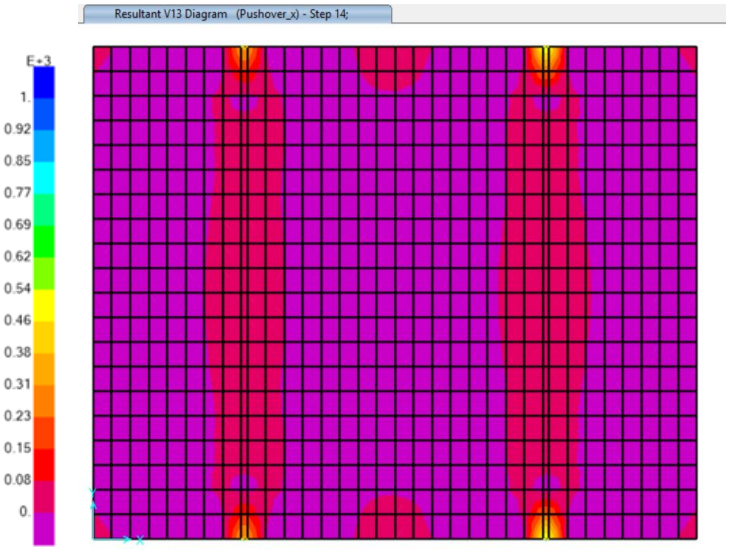

Figure 57 Shear V13: model with 15 cm thick slab

To account for the effect of post-tensioning, the design values provided in the precast company's catalogue were adopted. The cross-section considered most representative for the verifications is the HSC160, as shown in Figure 58.

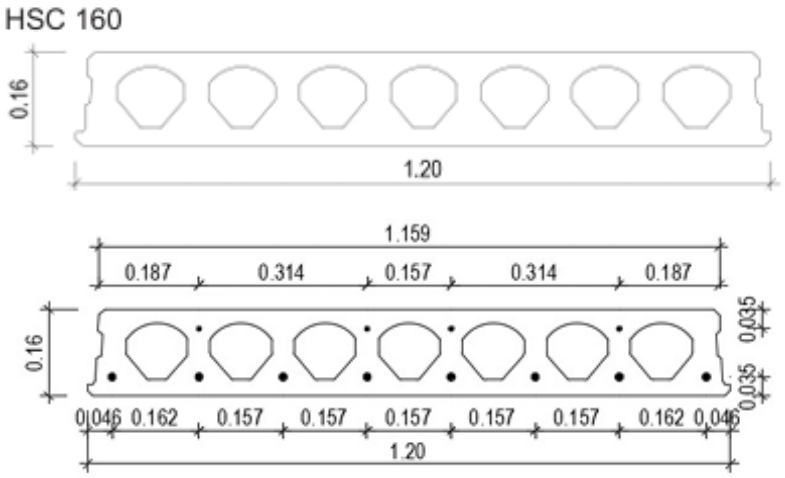

Figure 58 Hollow-core sections

Quadro de Propriedades para Dimensionamento

Laje	Lâmina de Compressão (mm)	Altura total (mm)	Peso (kg/m²)	Nº Cordões inferior	EI (kN.m²/m)	M_{rd} (kN.m/m)	M_{fctk} (kN.m/m)	V_{rd} (KN/m)	$AS_{dist.}$ (A500) (cm²/m)	AS_{apoios} (A500) (cm²/m)	Consumo Lâmina de Comp. (m³/m²)
HSC160+50	50	210	399	4	23274	74.92	50.00	77.83	2.31	1.73	0.059
				6	21946	102.17	63.17	80.25	3.46	2.59	
				8	20619	125.25	72.75	82.42	4.61	3.46	
HSC160+80	80	240	476	4	36364	90.08	55.92	78.83	2.31	1.73	0.089
				6	34604	125.25	73.83	81.58	3.46	2.59	
				8	32904	153.58	87.42	83.83	4.61	3.46	
HSC160+100	100	260	527	4	45588	100.33	58.75	79.17	2.31	1.73	0.109
				6	43602	138.50	80.08	82.00	3.46	2.59	
				8	41646	172.50	96.67	84.33	4.61	3.46	
HSC160+120	120	280	577	4	56216	110.50	60.67	79.25	2.31	1.73	0.129
				6	53976	153.00	85.50	82.17	3.46	2.59	
				8	51735	191.25	105.50	84.58	4.61	3.46	

Figure 59 Precast company table

By combining the verification rules of Eurocode 2 with the catalogue data, and after satisfying the checks for the two considered limit cases, the final model was defined as a one-way slab represented by a single shell element with an equivalent thickness of 15 cm, corresponding to the shear-effective depth.

5 VALIDATION OF EXPERIMENTAL TEST OF THE VERTICAL CONNECTION

The following chapter presents the modelling strategies adopted in order to reproduce the experimental tests as accurately, followed by a discussion of the numerical results and their comparison with the experimental results. The tests were carried out to investigate the behaviour of the vertical connections and to assess how adequate detailing in the vicinity of the joint influences their structural performance.

In order to achieve a more accurate representation of the tested specimen, the structural model in SAP2000 was developed using layered shell elements, allowing for the differentiation between the solid concrete portion, the insulation layer, and the reinforcing mesh described in Section 3.3. This approach ensured that the heterogeneous composition of the panel was properly reflected in the numerical simulation. For the reinforcement of Type 2, the bars were modelled using frame elements with an equivalent thickness. Axial plastic hinges were assigned along the entire length of these frame elements to capture potential yielding under axial forces.

The vertical connection was modelled using a nonlinear Plastic-Wen link, connected to the concrete specimen via a frame element representing the steel plate. The nodes of this frame were assigned Equal Z constraints, allowing the stresses to be properly distributed across the connection and ensuring realistic force transfer between the vertical connection and the precast wall.

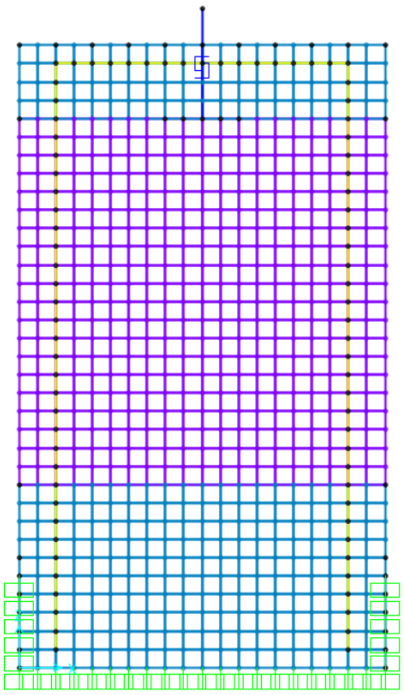

Figure 60 Specimen

The results obtained for Group 2 are presented below. It can be observed that a strut-and-tie mechanism develops, with cracks forming along the tensile ties (concrete) when the maximum force recorded in the experimental test is considered. This behaviour is evident both in the experimental tests (Figure 61) and in the numerical model (Figure 62 and Figure 63). Finally, the force–displacement curve derived from the numerical analysis is reported and compared with the one obtained from the experimental tests (Figure 64).

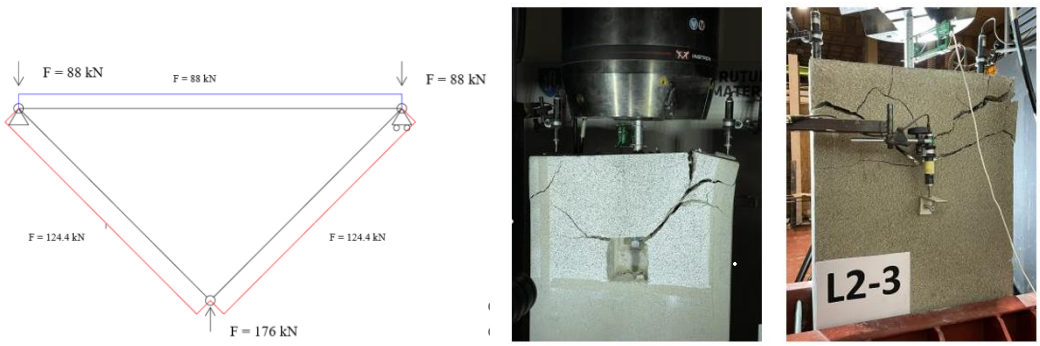

Figure 61 a) Strut-and-Tie (Group 2) b) Failure mode Group 2 (Figure from [36])

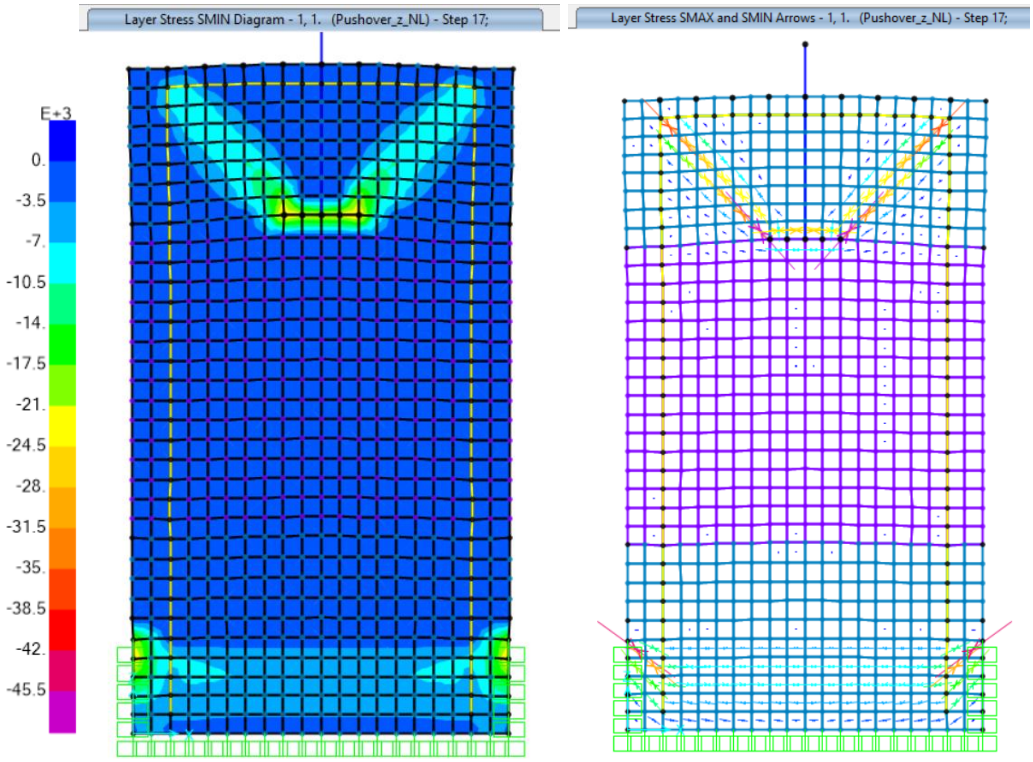

Figure 62 Stress in the concrete layer (Group 2)

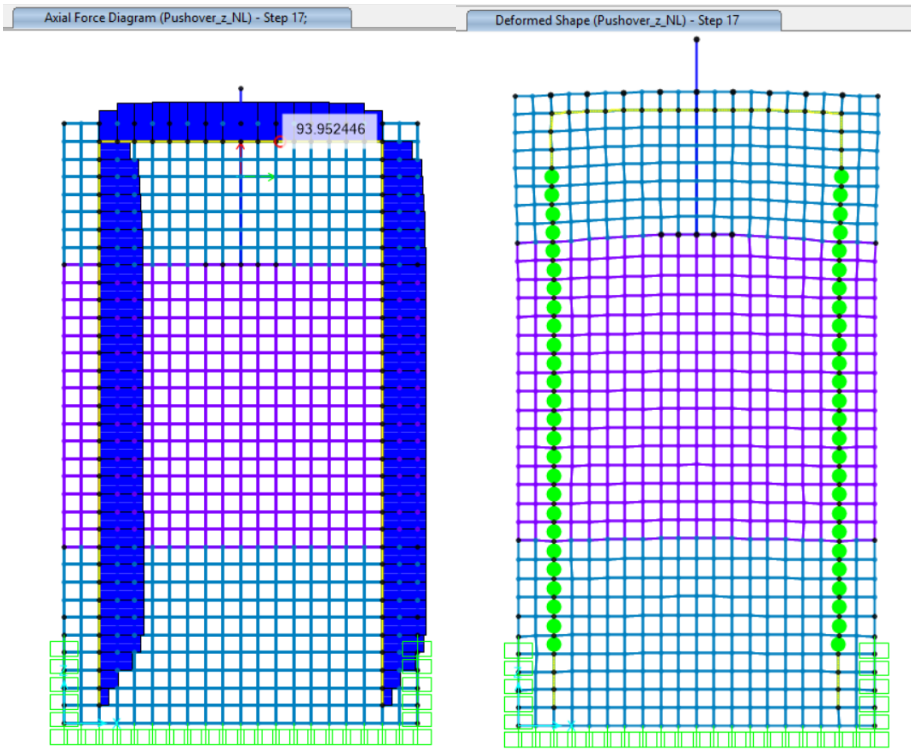

Figure 63 Axial force and plastic hinges in additional reinforcement bars (Group 2)

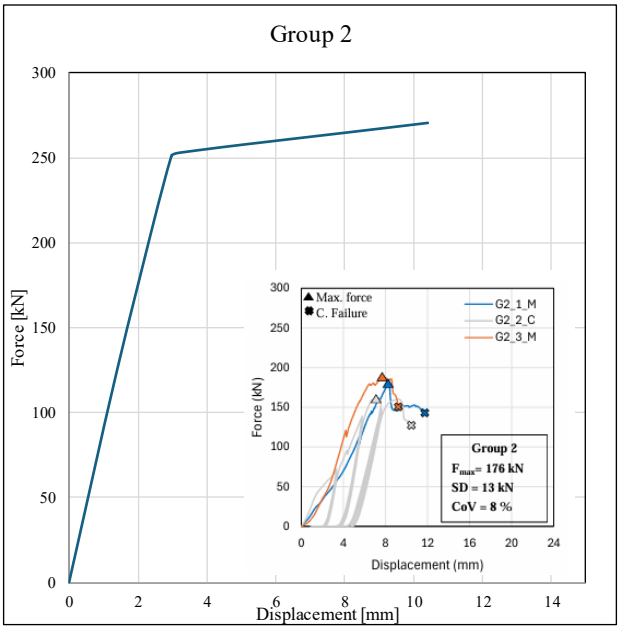

Figure 64 Force-displacement (Group 2)

For Groups 3, 4, and 6, only the force–displacement curves are reported, presented in comparison with those obtained from the experimental tests.

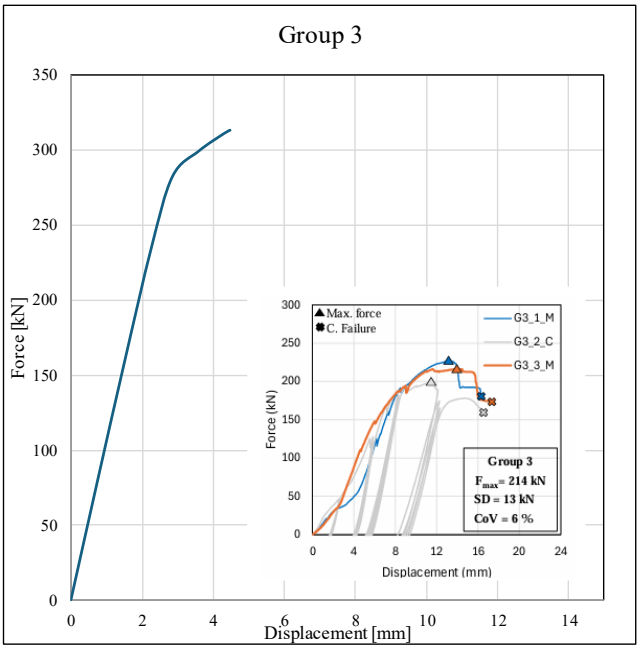

Figure 65 Force-displacement (Group 3)

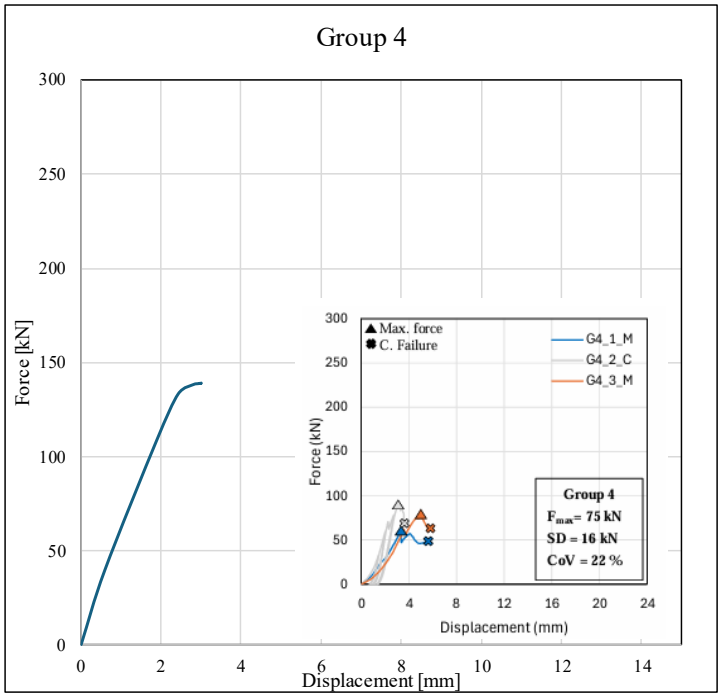

Figure 66 Force-displacement (Group 4)

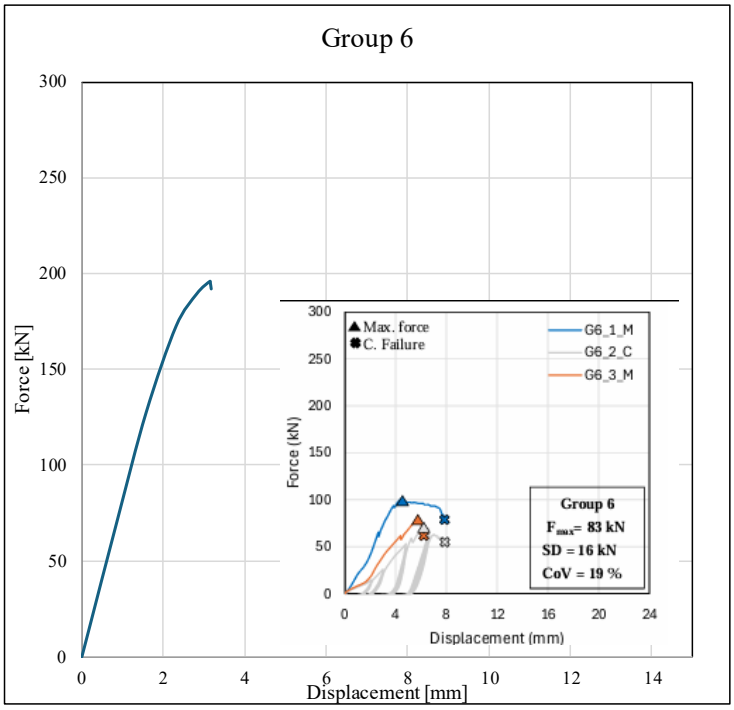

Figure 67 Force-displacement (Group 6)

Some simplifications were made in the modelling process: the hole was not explicitly modelled, and perfect bond between concrete and reinforcement was assumed. Despite these assumptions, the model is considered sufficiently accurate to capture the overall behaviour of the vertical connection. Both the experimental and numerical results indicate that, in order to concentrate the damage within the vertical connection, a smaller diameter for the connection elements should be considered.

The following sections present the analyses carried out on both the simplified model and the full building model, considering the previously discussed results and, consequently, adopting a reduced connection diameter of 25 mm to ensure the concrete cracking.

6 ANALYSIS OF SMALL BUILDING MODEL

Basically, two types of analysis could be used to examine the seismic behaviour of the wall-system, a dynamic analysis or a static analysis.

In this study, the seismic vulnerability assessment of the small building was conducted through three types of numerical analyses. Modal analysis was first performed to determine the natural frequencies and the corresponding vibration modes of the structure. Subsequently, nonlinear pushover and nonlinear dynamic analyses were carried out, to evaluate the capacity curves and parameters such as initial stiffness, maximum strength, inter-storey drift profiles and the performance points. Nonlinear dynamic analyses were executed since the representation of seismic events is very accurate in terms of their effects and the response behaviour of the building.

6.1 MODAL ANALYSIS

Modal analyses are significant for identifying the natural frequencies and mode shapes of the structure, which allows the understanding of the dynamic characteristics of the building. Each structure exhibits its unique oscillatory behaviour, even in the absence of external forces, at specific frequencies, which are associated with distinct deformation patterns known as mode shapes. Moreover, characterizing the natural frequencies and mode shapes provides valuable insights into the vibrational response of buildings during earthquakes, allowing for a more accurate prediction of their behaviour and the detection of vulnerable regions that may require reinforcement.

The Eurocode 8 highlights in the section related to modal analysis that the sum of the effective modal mass for the considered modes represents, at least, 90% of the total mass of the structure.

The periods obtained from the modal analyses are presented in Table 4 and the corresponding vibration modes are presented in Figure 68.

TABLE: Modal Participating Mass Ratios						
OutputCase	**StepType**	**StepNum**	**Period**	**UX**	**UZ**	**RY**
Text	Text	Unitless	Sec	Unitless	Unitless	Unitless
MODAL	Mode	1	0.1155	77%	0%	21%
MODAL	Mode	2	0.0384	18%	0%	59%
MODAL	Mode	3	0.0357	0%	87%	0%
MODAL	Mode	4	0.0245	1%	0%	0%
MODAL	Mode	5	0.0217	0%	0%	0%
MODAL	Mode	6	0.0201	3%	0%	11%
MODAL	Mode	7	0.0188	0%	7%	0%
MODAL	Mode	8	0.0181	0%	0%	0%
MODAL	Mode	9	0.018	0%	0%	0%
MODAL	Mode	10	0.0173	0%	0%	0%
MODAL	Mode	11	0.0173	0%	1%	0%
MODAL	Mode	12	0.0172	0%	0%	1%

Table 4 Modal analyses small building: Periods and participating mass ratios

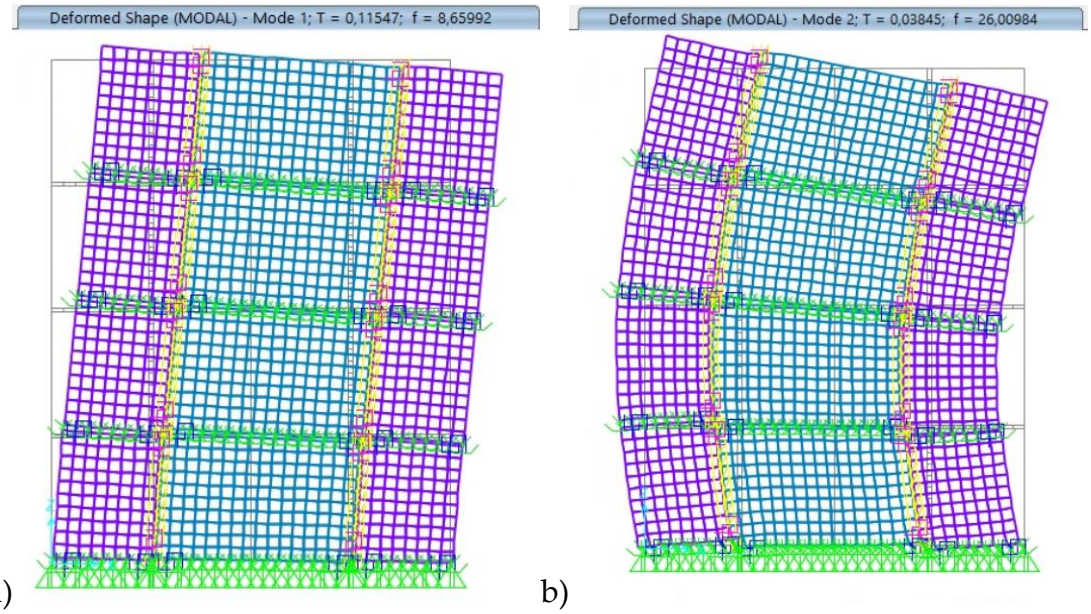

Figure 68 Vibration modes: a) First mode; b) Second mode

6.2 EXPECTED MAXIMUM DISPLACEMENT

For an accurate modelling of the vertical connections, two potential global mechanisms that can develop in this type of precast wall buildings were identified: rocking and sliding.

The rocking mechanism occurs when the wall panels behave as rigid blocks that rotate around their base corners under lateral loading. In this case, the uplift and compression at the opposite edges of the wall govern the response, and the connections mainly experience tension and compression forces (Figure 69). Assuming small rotation angles and a known top displacement, the elongation of the vertical connection can be expressed as:

$$\delta = \frac{b}{h} \cdot \Delta \tag{1617}$$

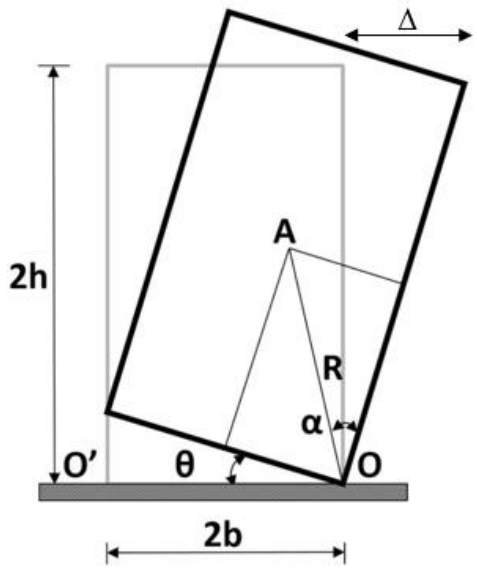

Figure 69 Rocking block geometry

The elongation of vertical connections becomes particularly relevant under cyclic loading, where it may affect the overall response of the structure.

Conversely, the sliding mechanism develops when the lateral loads cause a relative horizontal displacement along the wall-to-foundation or wall-to-wall interfaces. In this case, shear forces are primarily resisted by the friction and shear capacity of the connections. Understanding which of these mechanisms prevails is crucial to correctly estimate the expected maximum displacement and to properly calibrate the nonlinear behaviour of the vertical connections in the numerical model.

Nonlinear static and dynamic analyses were therefore performed to accurately evaluate the governing mechanism.

6.3 NONLINEAR STATIC PUSHOVER ANALYSIS

This type of analysis is commonly employed to evaluate the expected seismic performance of existing structures. The non-linear static (push-over) analysis was carried out assuming a "uniform" acceleration profile along the height of the structure, resulting in lateral forces proportional to the mass distribution (with loads applied at the top of each panel in the model). This loading pattern is one of the two distributions typically prescribed by seismic design codes (the other being triangular) and was adopted here as it is generally more demanding and more consistent with the deformation behaviour of the very stiff wall system under consideration. The horizontal loads were incrementally increased until a displacement of 6 cm was reached at the top-right corner of the wall system (control joint). In terms of drift ratio, this corresponds to a value of approximately

0.5%, which preliminary analyses indicated to exceed the actual deformation capacity of the system.

This analysis was first performed on a simplified two-dimensional model, where several parametric studies (different connections type, nonlinear material) were conducted to calibrate the numerical representation and ensure that it reflected the actual structural behaviour as closely as possible (see Section **Errore. L'origine riferimento non è stata trovata.**). Following these preliminary investigations, the need for a three-dimensional model became evident to capture the global response of the system with greater accuracy.

6.3.1 2D Analysis

The first step consisted in examining the behaviour of the three different types of proposed bolted connections. Based on this comparison, connection type 1 was selected for all subsequent analyses, as it proved to be the most practical solution in terms of capacity and assembly and disassembly, a fundamental requirement for this kind of prefabricated system (Figure 70).

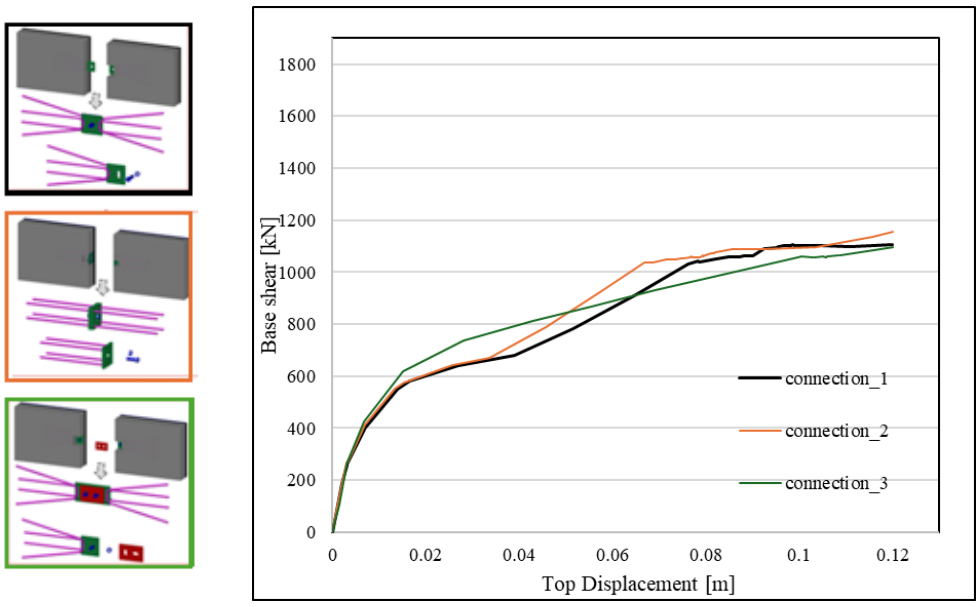

Figure 70 Comparison of capacity curves for the proposed bolted connection types

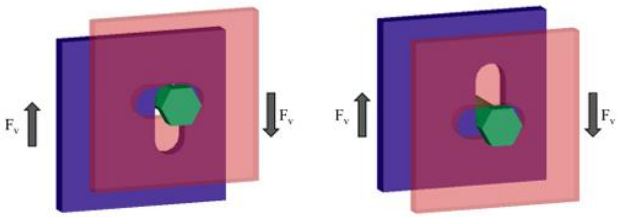

Figure 71 Displacement between steel plates due to ovalized holes on connections (Figure adapted from [38])

The second step then involved assessing the need to model the initial slack observed in the experimental tests on the horizontal connections of the vertical interface (shown in Section 4.2.3). As illustrated in Figure 72, it was found that both the influence of the connections on the interface and the slack caused by the oval-shaped holes (Figure 71), were found to play a significant role in the overall behaviour.

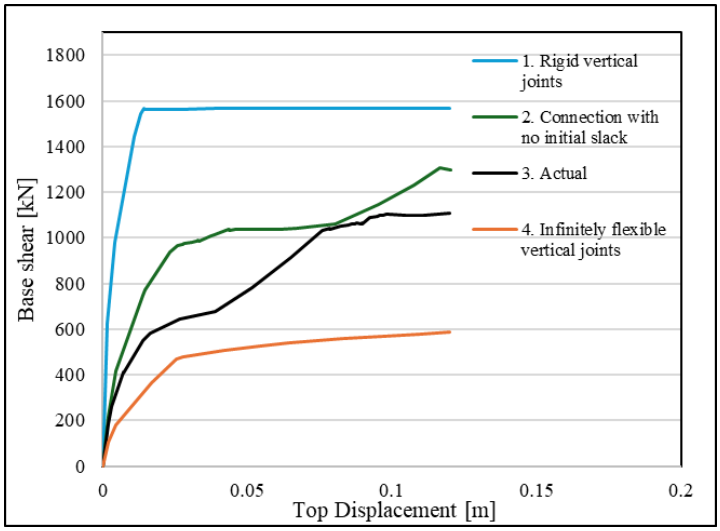

Figure 72 Capacity curves obtained from different modelling approaches for the vertical interface

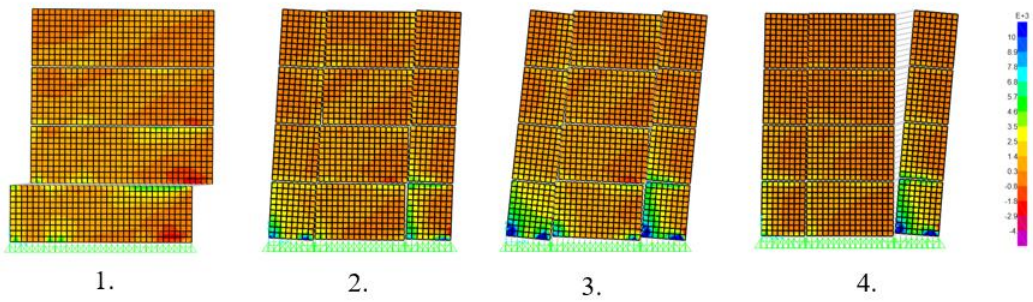

Figure 73 Deformed shape: shell stresses in concrete layer

Considering the results obtained, it became evident that considering a single wall did not adequately capture the global capacity of the system, as each wall alignment exhibited an independent behaviour. Consequently, the modelling approach was extended to include two walls connected through the floor slab, allowing for a more representative simulation of the overall structural response.

6.3.2 3D Global Analysis

In Section 4.3, the modelling choices and verifications carried out for the floor system are presented in detail. This section presents the results obtained with the final modelling choice, where the floor was represented as a 15 cm thick shell element with linear elastic properties. By accounting for the diaphragm action of the slab on the wall panels, it emerges that the influence of the connections on the vertical interface is minimal. For this reason, the investigation was further developed through a parametric study to explore the global behaviour of the system.

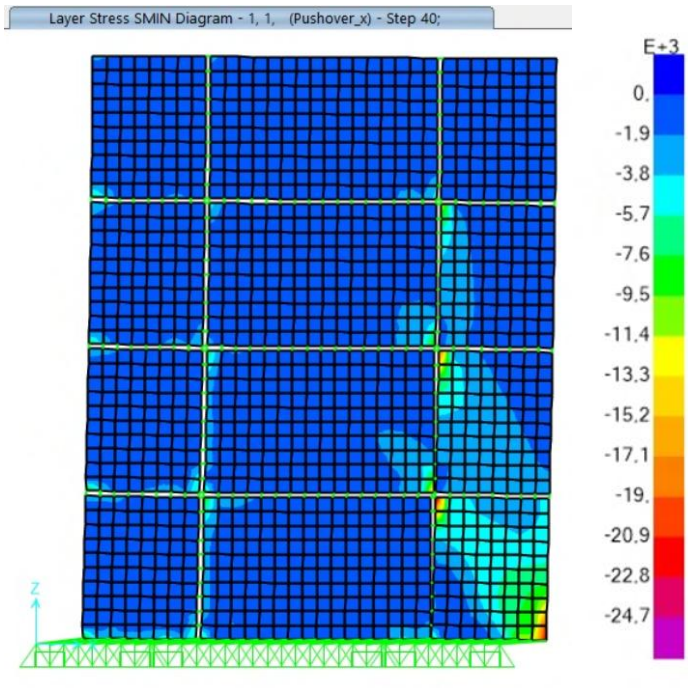

Figure 74 Deformed Shape: sliding mechanism at the base

The deformed shape of the building indicates that sliding occurs predominantly at the base. This localized sliding is mainly attributed to the force distribution adopted in the pushover analysis, which was defined as uniform along the building height The results of the capacity curve, shown in Figure 75, illustrate the contributions of the connections along the horizontal interface. Since sliding is concentrated at the base, the contribution of friction is significant, as is the shear resistance of the connections, leading to an ultimate lateral capacity of approximately 67% of the building's total weight.

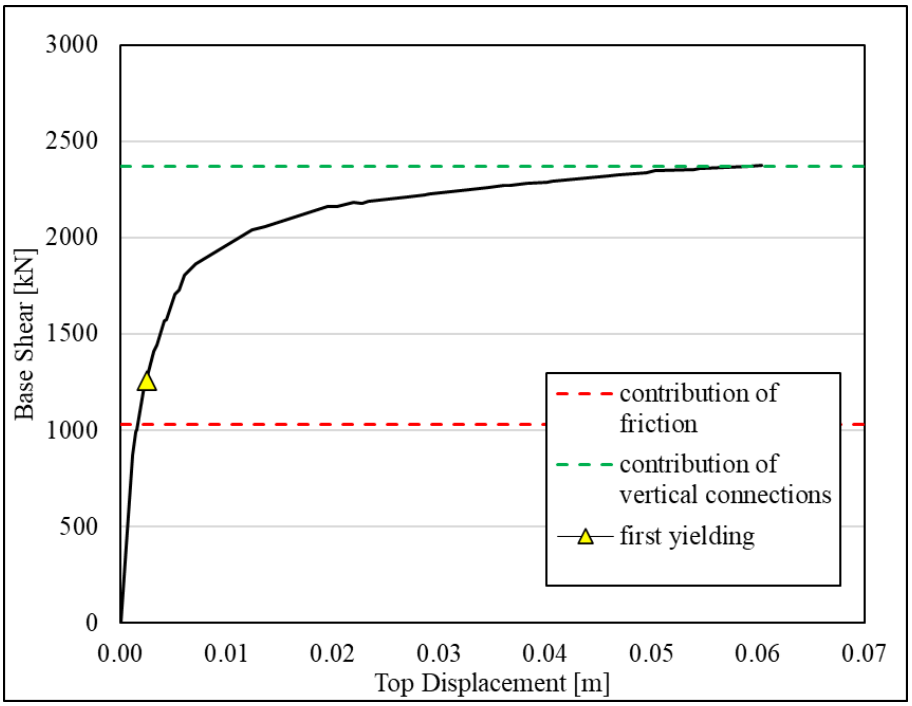

Figure 75 Pushover curve: small building

6.3.2.1 Effect of the Reinforcement Mesh Diameter

Up to this point, the results have been presented assuming wall panels with elastic behaviour. Consequently, it became necessary to verify whether the nonlinear behaviour of the concrete in the panels should be explicitly modelled, and to perform a sensitivity analysis on the diameter of the reinforcement mesh bars. The results obtained from this investigation are illustrated in Figure 76.

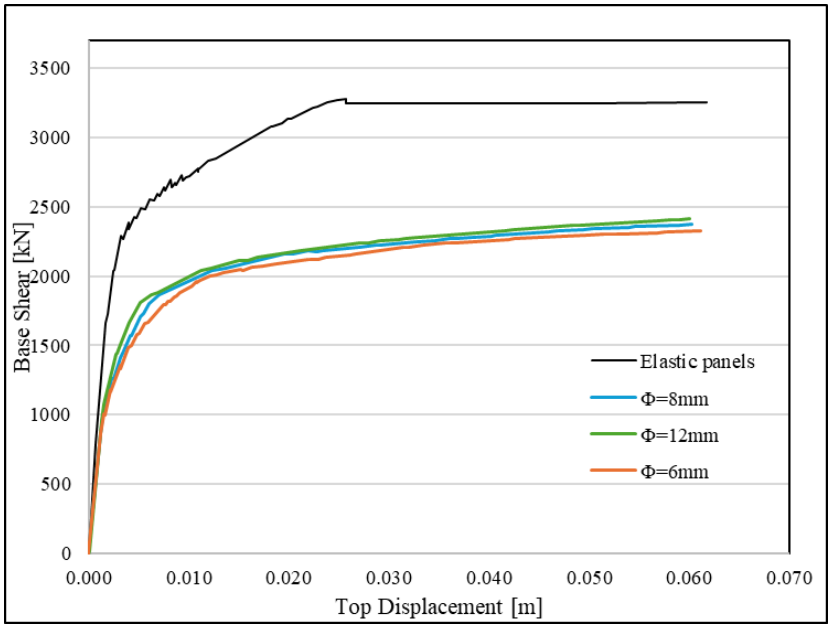

Figure 76 Sensitivity of reinforcement mesh diameter

From the results, it emerged that, contrary to initial expectations, the contribution of the concrete within the panels is significant and cannot be neglected. Therefore, for the subsequent analyses, the panels were modelled with nonlinear coupled behaviour, described in Section 4.1, and reinforced using a mesh of ϕ8/100.

6.3.2.2 Effect of Friction

A sensitivity analysis was conducted to investigate the influence of the friction coefficient between the concrete-to-concrete contact surfaces of adjacent panels. A series of pushover analyses were performed considering different values of the friction coefficient μ. The results, shown in Figure 77, revealed that the friction coefficient has a significant impact on the overall structural response of the system.

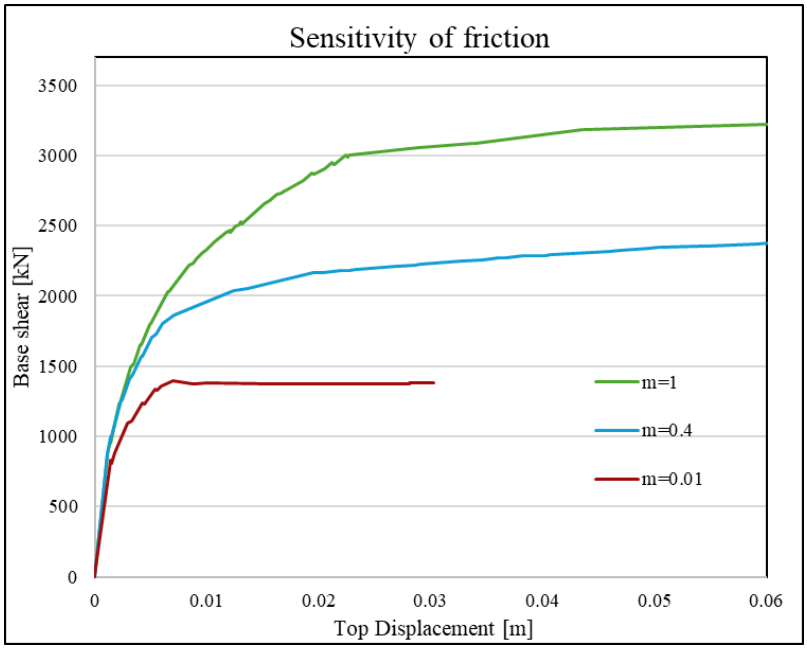

Figure 77 Sensitivity of friction

Friction significantly affects the load transfer mechanism between adjacent panels by altering the balance between shear transfer through the vertical reinforcement bars and direct shear resistance developed at the concrete-to-concrete interface. In fact, when a zero-friction coefficient ($\mu \cong 0.01$) is assumed, the global shear capacity is governed by the contribution of the vertical connections alone, as the interface is unable to mobilize any appreciable frictional resistance. In the subsequent analyses, a friction coefficient of $\mu = 0.4$ was adopted, in accordance with the model proposed by Tsoukantas and Tassios [41]. Therefore, the role of friction represents a key aspect that warrants further investigation in future research.

6.4 NONLINEAR DYNAMIC ANALYSIS

To provide a more realistic assessment of the seismic performance of the proposed precast wall system, nonlinear dynamic analyses (time history) were carried out. Unlike static or simplified approaches, this method explicitly captures the time-dependent response of the structure under earthquake ground motions, accounting for material nonlinearities as well as the complex interaction between walls, connections, and slabs. This type of analysis is particularly relevant for evaluating global stability and potential damage mechanisms under realistic seismic conditions.

An accelerogram recorded during the L'Aquila earthquake was selected as input ground motion. This record was deliberately chosen for its relatively smooth characteristics, without abrupt peaks, to avoid potential convergence issues in the numerical model (Figure 78). Viscous damping was modelled using Rayleigh proportional damping, calibrated to correspond to 5% at the periods of the first and second vibration modes of the structure.

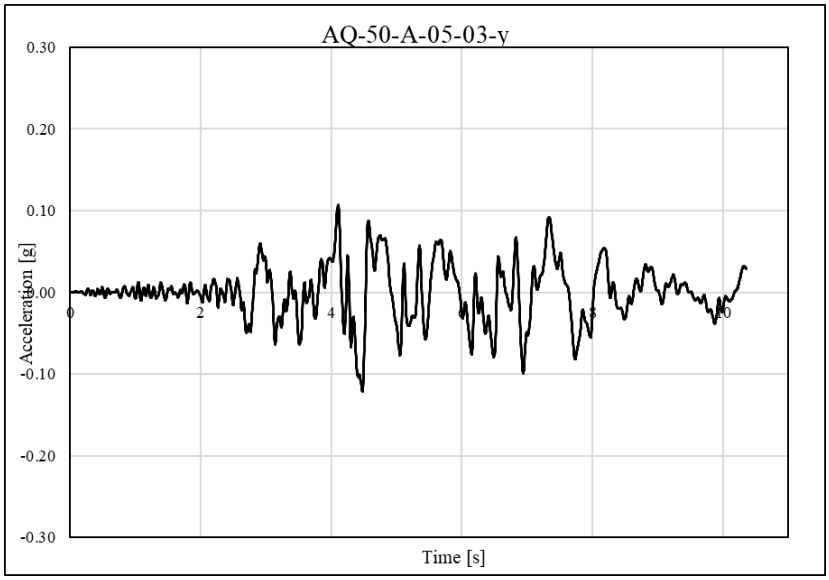

Figure 78 Record L'Aquila

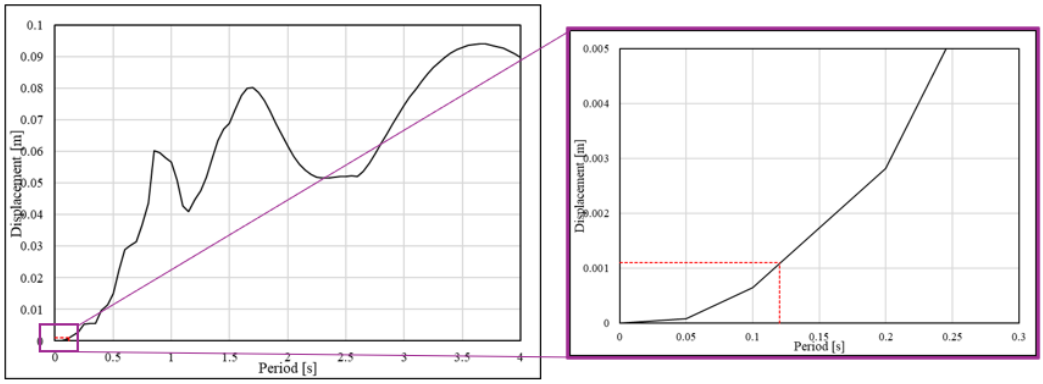

Figure 79 Elastic Displacement spectrum

By entering the fundamental period of the structure into the displacement response spectrum (Figure 79) of the selected ground motion, it can be observed that the expected displacement demand is approximately 1 mm. The selected accelerogram was scaled by factors ranging from 1 to 3 to generate input motions with different peak ground accelerations (PGA). The corresponding structural responses were then compared in terms of maximum top displacement, base shear, and overall deformation pattern, to evaluate the influence of increasing seismic intensity on the global behaviour of the system.

The results are presented for Node 237, located at the top of the structure, and for Link 504 at the base, which was identified as one of the most critical connections in terms of demand.

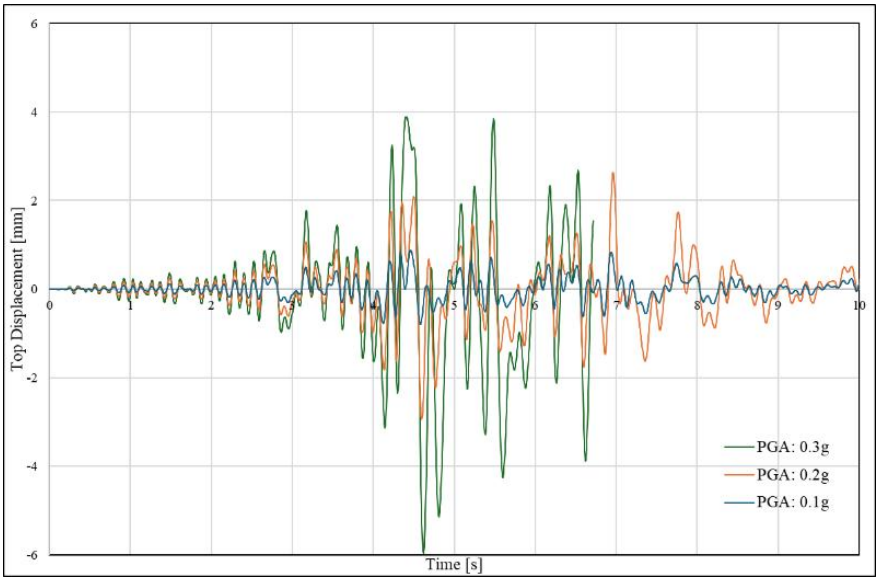

Figure 80 Displacement joint 237 (top)

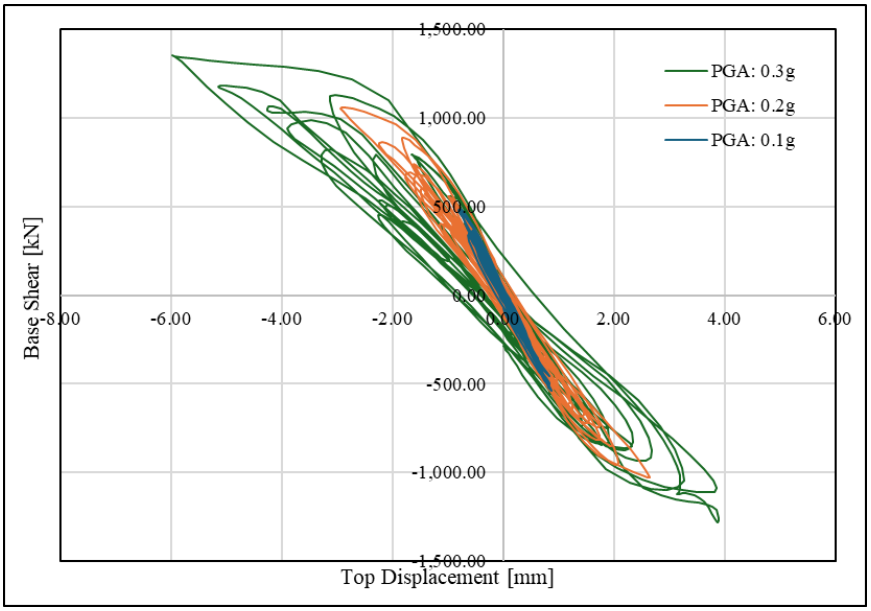

Figure 81 Base Shear – Top Displacement

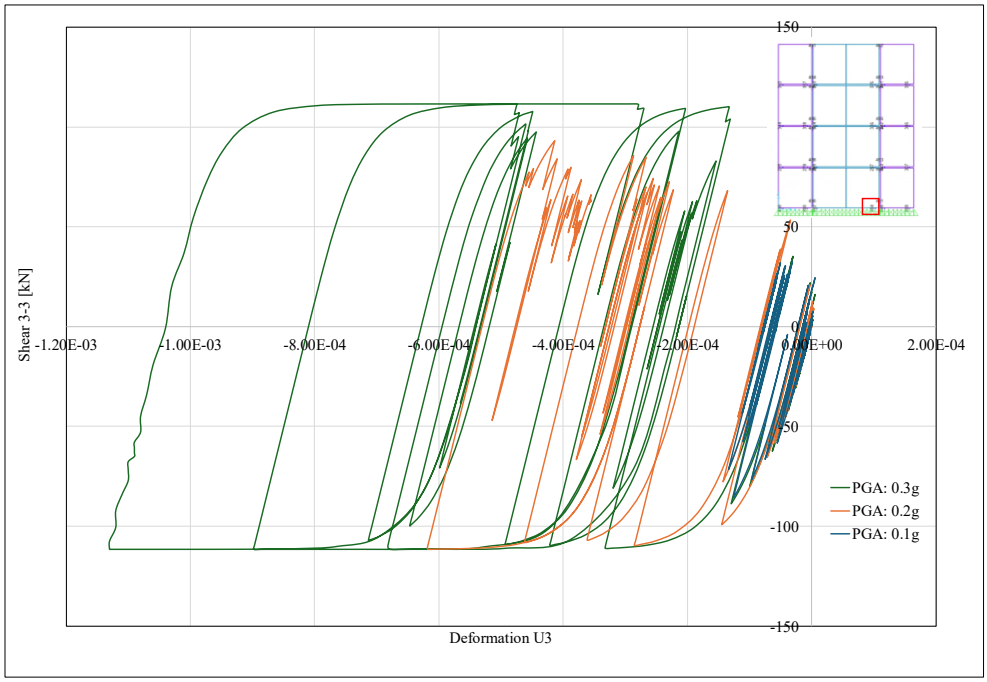

Figure 82 Shear Force-Deformation U3 (Vertical connection: Link 504)

As expected, the results of the nonlinear dynamic analysis confirmed that the predominant failure mechanism is the horizontal sliding between the panel horizontal interfaces, mainly concentrated at the base of the wall system. Conversely, the vertical interfaces exhibited no appreciable relative displacement, confirming that the shear connectors along these joints play a marginal role in the global load transfer mechanism.

As shown in Figure 83, the variation of the interstorey drift ratio for the different intensity levels of the input motion demonstrates that the overall drift pattern remains nearly unchanged with increasing seismic intensity. The maximum interstorey drift is observed at the second floor, where relative displacements between panels are more pronounced.

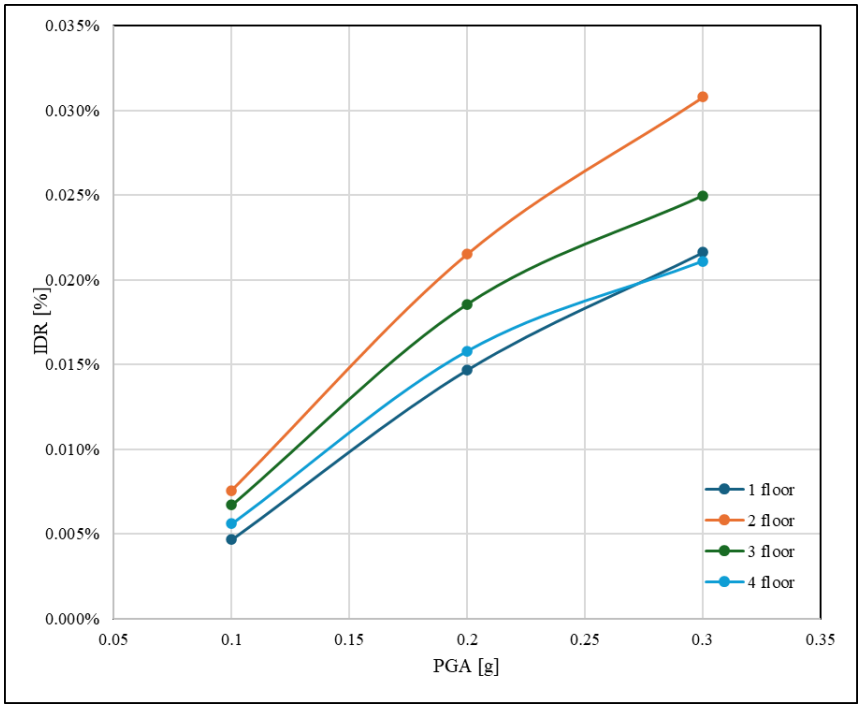

Figure 83 Interstorey Drift Ratio for the different levels

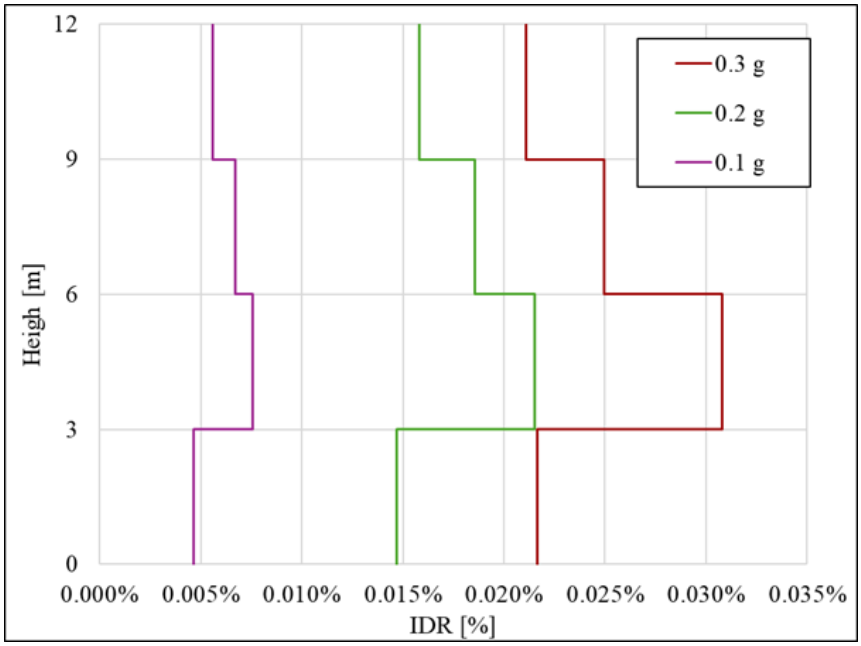

Figure 84 IDR

Unlike the findings from the static pushover analysis, the dynamic analysis allowed us to observe the actual damage mechanism, which is sliding primarily between the first and second storeys rather than being concentrated at the base.

This discrepancy is likely due to the oversimplified definition of the lateral load pattern adopted in the pushover analysis.

Finally, the stress distribution in the concrete panels reveals a localized concentration of stresses in the vicinity of the vertical connections. However, these values remain below the concrete tensile strength, indicating that no cracking or significant damage is expected to occur in the panels under the applied seismic loading.

It would have been interesting to assess the vertical component of the seismic excitation, as both static and nonlinear dynamic analyses have shown that the main damage mechanism is sliding, which is particularly influenced by friction and, consequently, by the normal forces. However, this evaluation was not performed in this thesis due to the high computational demand, which is already around 24–30 hours for the horizontal component. It is left for future studies, possibly using more suitable software.

7 PERFORMANCE ASSESSMENT OF FULL BUILDING TO EN1998

After validating the simplified model, the analysis was extended to the full modular building to evaluate its seismic performance in compliance with Eurocode 8 (EN 1998). Based on the results obtained from the previous sections, the model incorporates the calibrated parameters for connections and materials to ensure a realistic representation of the structural response. The performance is evaluated in terms of capacity curves and inter-storey drift ratios.

7.1 DESCRIPTION OF THE EXANIMATED BUILDING

The following section presents the four-storey building considered for the performance assessment, illustrated in Figure 85, with the corresponding plan type layout shown in Figure 86. Three different types of wall panels were identified: external insulated load-bearing panels with a total thickness of 40 cm (10 cm + 20 cm + 10 cm), internal insulated load-bearing panels with a total thickness of 24 cm (8 cm + 8 cm + 8 cm), and panels with openings such as doors and windows. In this model, the wall panels were represented considering only the inner concrete layers, with the insulation core surrounded by a full concrete layer along the perimeter. In the connection between orthogonal panels, no shear connectors were defined and only contact links were modelled.

For the modelling of the connections, floor system, applied loads, and materials the same assumptions and modelling choices adopted for the simplified model, described in the previous sections, were followed.

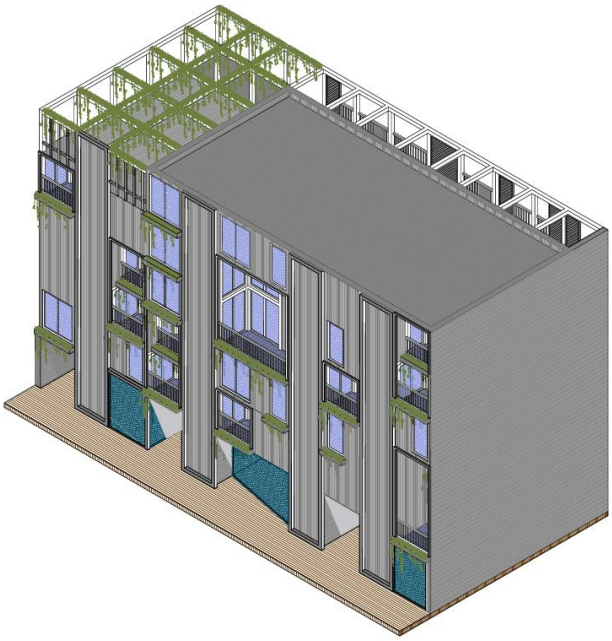

Figure 85 3D view of the residential building

The structure includes two stairs and lift shafts positioned at both ends of the building. Regardless, these portions of the building were not considered as the intention is to verify if a whole precast structure has the strength to withstand lateral forces by itself, without the need of any structural nucleus.

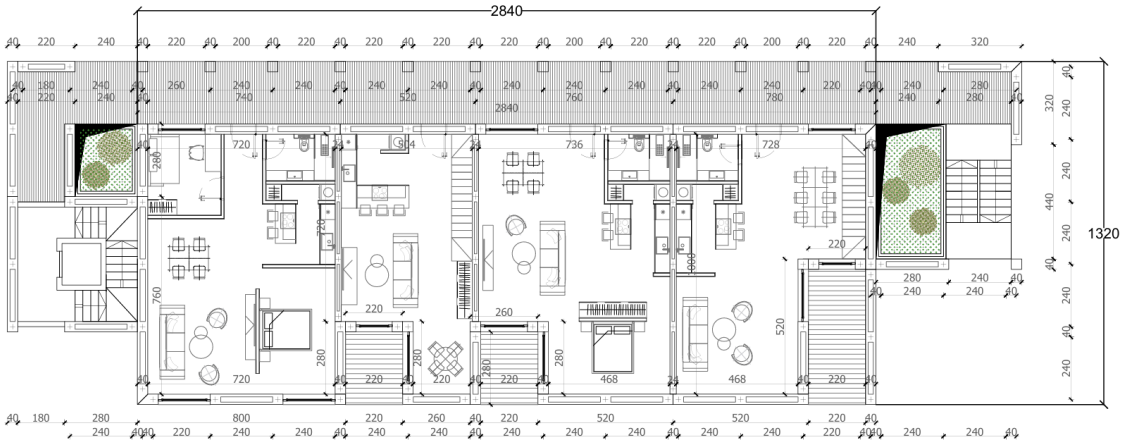

Figure 86 Standardized plan floor configuration

7.2 MODAL ANALYSIS

A modal analysis was performed on the full building model to identify the natural frequencies, periods and mode shapes of the structure. Figure 87 presents the fundamental vibration modes in the two principal translational directions (Ux and Uy), while Table 5 reports the corresponding natural periods and participating mass ratios. The identified modal shapes were therefore adopted as reference shapes for the pushover analyses described in the following section.

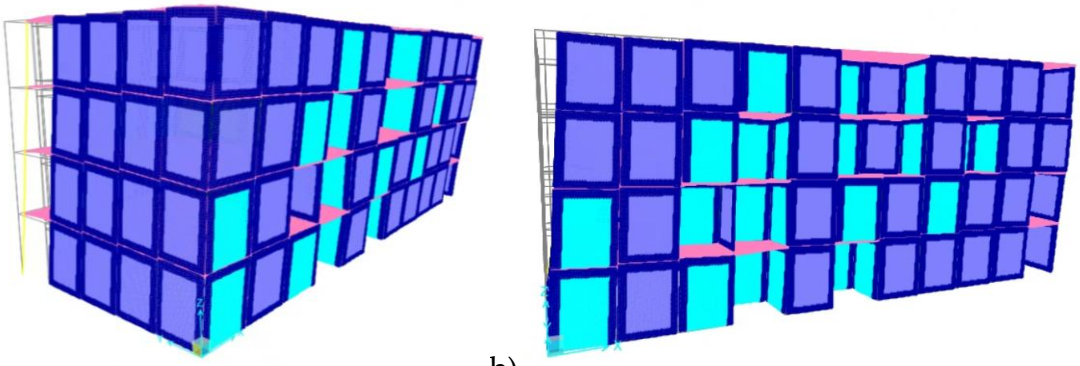

a) b)

Figure 87 Vibration modes: a) First mode; b) Fourth mode

TABLE: Modal Participating Mass Ratios						
OutputCase	**StepType**	**StepNum**	**Period**	**UX**	**UY**	**RZ**
Text	Text	Unitless	Sec	Unitless	Unitless	Unitless
MODAL	Mode	1	0.111	8%	69%	3%
MODAL	Mode	2	0.11	0%	0%	0%
MODAL	Mode	3	0.108	3%	1%	1%
MODAL	Mode	4	0.108	52%	10%	15%
MODAL	Mode	5	0.099	0%	0%	0%
MODAL	Mode	6	0.097	11%	0%	38%
MODAL	Mode	7	0.097	7%	0%	23%
MODAL	Mode	8	0.094	0%	0%	0%
MODAL	Mode	9	0.094	0%	0%	0%
MODAL	Mode	10	0.093	0%	0%	0%
MODAL	Mode	11	0.091	0%	0%	0%
MODAL	Mode	12	0.09	0%	0%	0%

Table 5 Modal analyses full building: Periods and participating mass ratios

The identified modal shapes were therefore adopted as reference shapes for the pushover analyses described in the following section.

7.3 PUSHOVER ANALYSIS

Differently from the simplified small building discussed in Section 6.3, for the full building model the nonlinear static (pushover) analyses were performed by applying lateral load patterns consistent with the translational modal shapes obtained from the previous modal analysis. These modal shapes, corresponding to the fundamental modes in the X and Y directions, were used to better represent the realistic distribution of inertia forces along the height of the structure. This approach allows for a more accurate estimation of the global seismic response and the identification of potential weak regions or failure mechanisms within the building.

Figure 88 and Figure 89 shows, the global relationship between base shear and top displacement of the wall-system and the horizontal displacement of the panels, for increasing intensity of the lateral forces for the two principal directions.

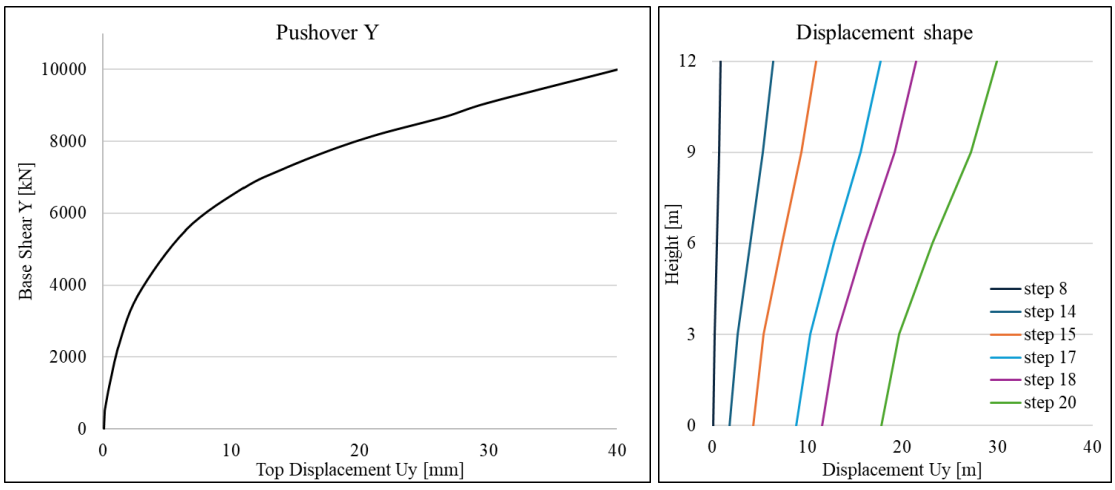

Figure 88 Left: push-over curve direction Y; Right: profiles of the lateral displacements along the height at different analysis steps

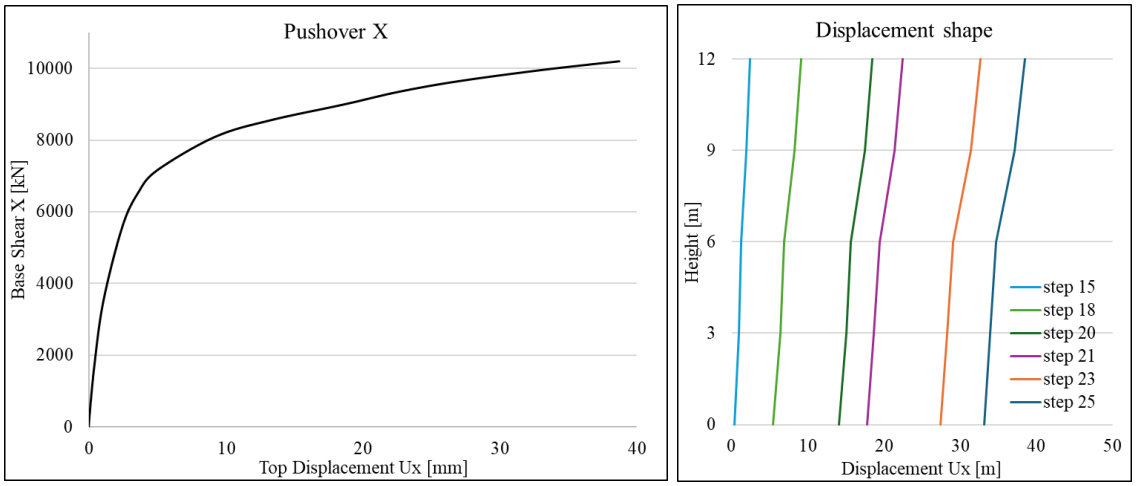

Figure 89 Left: push-over curve direction X; Right: profiles of the lateral displacements along the height at different analysis steps

In addition to the global capacity assessment, a detailed evaluation of the force contributions at each storey and at the base was carried out (Table 6 and Table 7). In particular, the relative roles of the vertical connections along the horizontal interfaces and the concrete-to-concrete friction were analysed to quantify their influence on the overall lateral resistance of the system (Figure 90). This allowed for a clearer understanding of how the different load transfer mechanisms interact and contribute to the global response under increasing lateral demand.

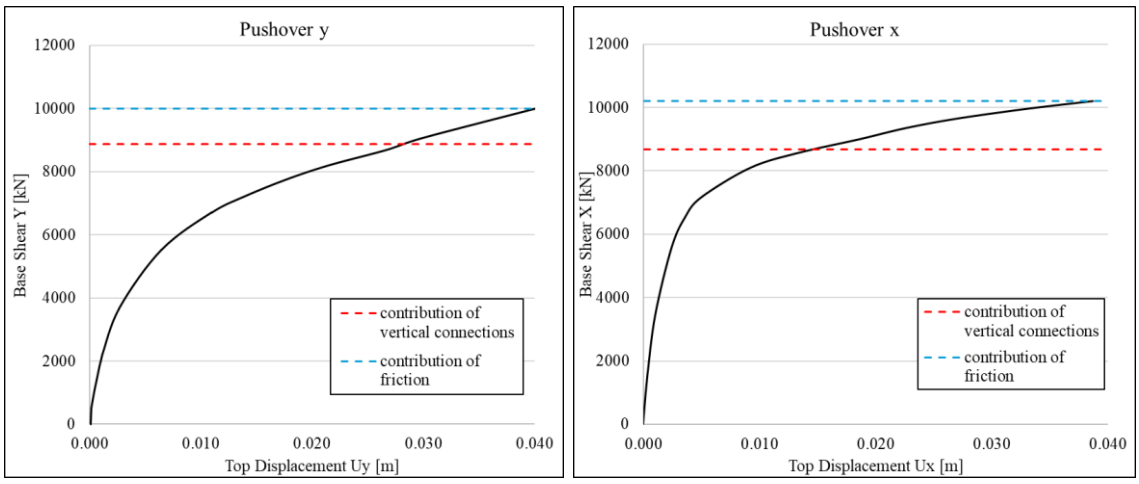

Figure 90 Force contribution

		vertical connection		friction link	
1 storey	*abs*	-8867.4	kN	-205.3	kN
	rel	97.7	%	2.3	%
2 storey	*abs*	-1396.3	kN	-1221.0	kN
	rel	53.3	%	46.7	%
3 storey	*abs*	-3956.1	kN	-2550.4	kN
	rel	60.8	%	39.2	%
4 storey	*abs*	-2426.4	kN	-1247.0	kN
	rel	66.1	%	33.9	%

Table 6 Force contribution: Pushover Y

		vertical connection		friction link	
1 storey	*abs*	8680.8	kN	1523.1	kN
	rel	85.1	%	14.9	%
2 storey	*abs*	2032.8	kN	1771.5	kN
	rel	53.4	%	46.6	%
3 storey	*abs*	4695.0	kN	2414.7	kN
	rel	66.0	%	34.0	%
4 storey	*abs*	2782.1	kN	1143.4	kN
	rel	70.9	%	29.1	%

Table 7 Force contribution: Pushover X

From the results, it was observed that the structural capacity is approximately the same in both directions, as expected, since the number of resisting elements is nearly equivalent along the two axes. Moreover, a higher contribution of friction was identified at the second and third storeys, where larger interstorey drifts occurs.

Once the damage mechanism was identified, the results were compared with the seismic demand corresponding to a site-specific condition. In this study, the city of L'Aquila, located in a high-seismicity region of Italy, was selected as the reference site for the evaluation. The target displacement was evaluated at a single control point located at the top of the structure and according to EN 1998-1 the yield force Fy *, which represents also the ultimate strength of the idealized system, is equal to the base shear force at the formation of the plastic mechanism.

The initial stiffness of the idealized system is determined in such a way that the areas under the actual and the idealized force, deformation curves are equal (Figure 91).

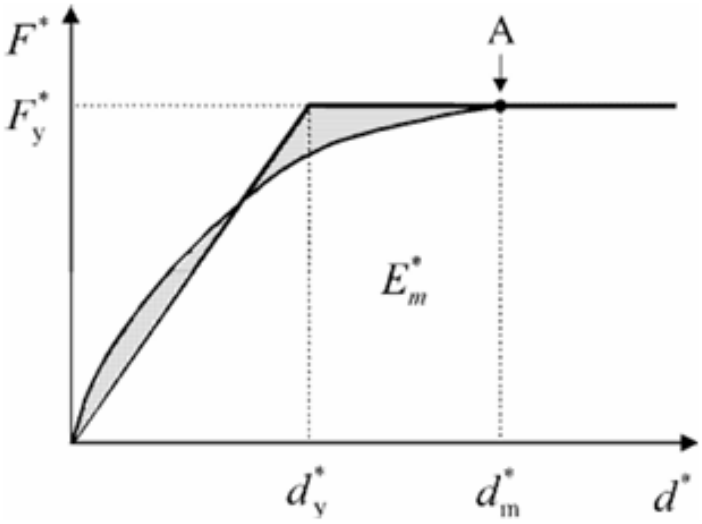

Figure 91 Determination of the idealized elasto - perfectly plastic force – displacement relationship (Figure adapted from [8])

Based on this assumption, the yield displacement of the idealised SDOF system dy * is given by:

$$d_y^* = 2\left(d_m^* - \frac{E_m^*}{F_y^*}\right) \tag{18}$$

Once the equivalent bilinear parameters were defined, the target spectral acceleration $S_e(T)$ was determined based on the period of vibration T_1 corresponding for simplicity at the period obtained by the modal analysis and the site-specific elastic response spectrum corresponding to L'Aquila.

$$S_e(T_1) = a_g \cdot S \cdot \left[1 + \frac{T_1}{T_B} \cdot (\eta \cdot 2{,}5 - 1)\right] \tag{19}$$

With

$a_g = 0.25\ g$ (SLV $T_R = 475\ years$)

$a_g = 0.33\ g$ (SLC: $T_R = 975\ years$)

$S = 1.2$ $(soil\ type\ B)$

$T_B = 0.15\ s$

$\eta = 1$

The corresponding spectral displacement $S_d$was then derived from:

$$d_{et}^* = S_e(T_1)\left[\frac{T^*}{2\pi}\right]^2 \quad (20)$$

For the determination of the target displacement dt * for structures in the short-period range, the following expression was employed:

$$d_t^* = \frac{d_{et}^*}{q_u}\left(1 + (q_u - 1)\frac{T_C}{T_1}\right) \geq d_{et}^* \quad (21)$$

Where qu is the ratio between the acceleration in the structure with unlimited elastic behaviour Se(T*) and in the structure with limited strength Fy * / m*.

$$q_u = \frac{S_e(T_1) * m}{F_y^*} \quad (22)$$

Figure 92 and Figure 93 present the results obtained for both directions, considering the Life Safety Limit State (SLV) with a return period of 475 years and the Near Collapse Limit State (SLC) with a return period of 975 years.

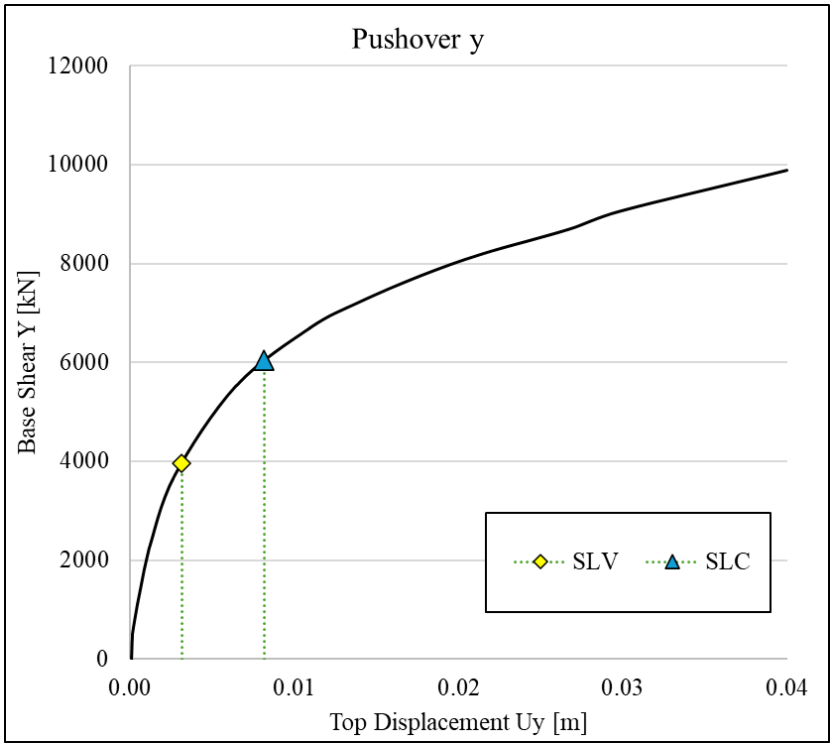

Figure 92 Target displacement: direction y

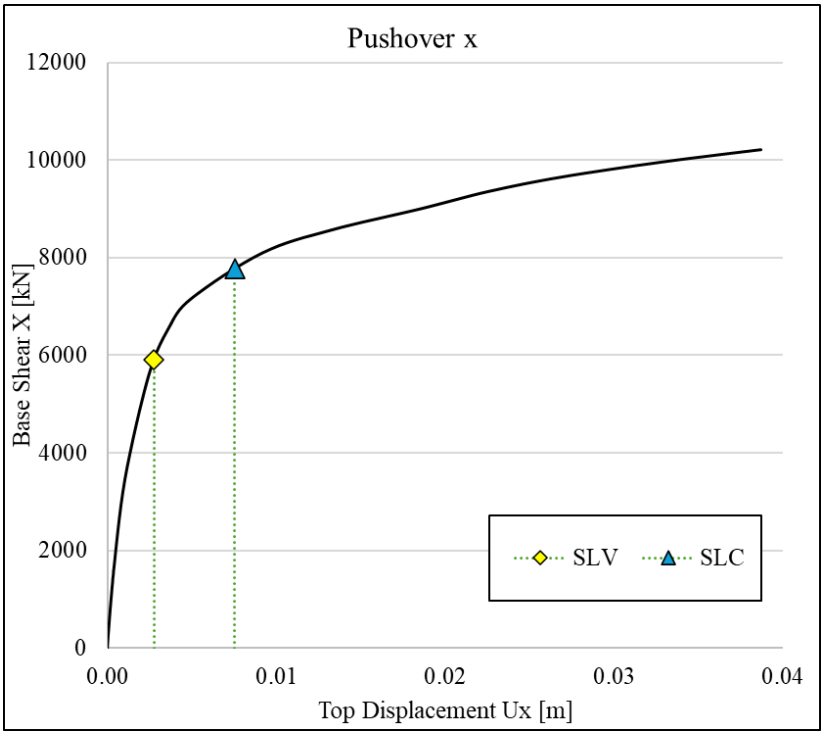

Figure 93 Target displacement: direction x

8 SUMMARY AND CONCLUSIONS

As stated in the Introduction, the purpose of this study was to examine the potentiality of a specific building prefabrication system patented in Portugal, to resist horizontal forces of the order of magnitude that could be expected in case of a seismic event.

The analysis revealed that the overall lateral capacity is predominantly governed by the horizontal interfaces, where interstorey sliding is concentrated, particularly at the first and second storeys, consistently across both models. In contrast, the horizontal connections along the wall-to-wall vertical interfaces contribute negligibly to the total base shear, confirming their secondary role in lateral load transfer. Despite the dominance of a sliding mechanism, relative displacements remained small (below 1 cm in the most critical cases) demonstrating that the system meets the performance criteria established by Eurocode 8.

The analyses also highlighted the critical sensitivity of the system to friction at the concrete-to-concrete interfaces, which strongly influences the balance between interface sliding and bar deformation. This pronounced influence is directly linked to the fact that the governing damage mechanism observed in the analyses was sliding at the horizontal interfaces. A nominal friction coefficient of $\mu = 0.4$ was adopted in accordance with Tsoukantas & Tassios; however, all assumptions regarding friction behaviour require validation through experimental evidence. Based on these key findings, several avenues for future research emerge.

In particular, a more refined assessment of friction is recommended, using nonlinear dynamic analyses that explicitly account for the vertical component of the earthquake, to capture fluctuations of normal forces at the interfaces and their effect on friction mobilization. Further investigation into the contribution of friction is suggested, including the potential use of Neoprene surfaces between panels to reduce this effect.

This system is continuously evolving, and ongoing tests are currently exploring the addition of shear-resistant connections at the horizontal interfaces between panels. The aim is to promote the activation of the rocking mechanism before sliding occurs, potentially enhancing energy dissipation.

The aim is to promote the activation of the rocking mechanism before sliding occurs, potentially enhancing energy dissipation. Another key aspect of prefabricated structures is reversibility, which allows connections to be easily removed and replaced following a seismic event. Although this feature is not critical for the current system—since the observed deformations and displacements do not necessitate it remains an important design consideration for prefabricated buildings, highlighting their potential for adaptability and rapid repair.

9 REFERENCES

[1] International Federation for Structural Concrete, Ed., *Seismic design of precast concrete building structures: state-of-art report*. in Bulletin / International Federation for Structural Concrete, no. 27. Lausanne: International Federation for Structural Concrete, 2003.

[2] FIB Bulletin 43, 'Structural connections for precast concrete buildings'. 2008.

[3] R. Sousa, N. Batalha, and H. Rodrigues, 'Numerical simulation of beam-to-column connections in precast reinforced concrete buildings using fibre-based frame models', *Eng. Struct.*, vol. 203, p. 109845, Jan. 2020, doi: 10.1016/j.engstruct.2019.109845.

[4] C. Casotto, V. Silva, H. Crowley, R. Nascimbene, and R. Pinho, 'Seismic fragility of Italian RC precast industrial structures', *Eng. Struct.*, vol. 94, pp. 122–136, July 2015, doi: 10.1016/j.engstruct.2015.02.034.

[5] F. Clementi, A. Scalbi, and S. Lenci, 'Seismic performance of precast reinforced concrete buildings with dowel pin connections', *J. Build. Eng.*, vol. 7, pp. 224–238, Sept. 2016, doi: 10.1016/j.jobe.2016.06.013.

[6] D.-C. Feng, G. Wu, and Y. Lu, 'Finite element modelling approach for precast reinforced concrete beam-to-column connections under cyclic loading', *Eng. Struct.*, vol. 174, pp. 49–66, Nov. 2018, doi: 10.1016/j.engstruct.2018.07.055.

[7] M. N. Kataoka, M. A. Ferreira, and A. L. H. De Cresce El Debs, 'Nonlinear FE analysis of slab-beam-column connection in precast concrete structures', *Eng. Struct.*, vol. 143, pp. 306–315, July 2017, doi: 10.1016/j.engstruct.2017.04.028.

[8] *Eurocode 8, design of structures for earthquake resistance*. London: British Standards Institution, 2005.

[9] N. M. L. Batalha, 'SEISMIC PERFORMANCE ASSESSMENT OF EXISTING PRECAST REINFORCED CONCRETE INDUSTRIAL BUILDINGS AND RETROFITTING SOLUTIONS'.

[10] L. Liberatore, L. Sorrentino, D. Liberatore, and L. D. Decanini, 'Failure of industrial structures induced by the Emilia (Italy) 2012 earthquakes', *Eng. Fail. Anal.*, vol. 34, pp. 629–647, Dec. 2013, doi: 10.1016/j.engfailanal.2013.02.009.

[11] D. A. Bournas, P. Negro, and F. F. Taucer, 'Performance of industrial buildings during the Emilia earthquakes in Northern Italy and recommendations for their strengthening', *Bull. Earthq. Eng.*, vol. 12, no. 5, pp. 2383–2404, Oct. 2014, doi: 10.1007/s10518-013-9466-z.

[12] P. Negro and G. Toniolo, *Design Guidelines for Connections of Precast Structures under Seismic Actions*. 2012. doi: 10.2777/37605.

[13] Y. C. Kurama *et al.*, 'Seismic-Resistant Precast Concrete Structures: State of the Art', *J. Struct. Eng.*, vol. 144, no. 4, p. 03118001, Apr. 2018, doi: 10.1061/(ASCE)ST.1943-541X.0001972.

[14] R. Martins, R. D. Carmo, H. Costa, and E. Júlio, 'A review on precast structural concrete walls and connections', *Adv. Struct. Eng.*, vol. 26, no. 14, pp. 2600–2620, Oct. 2023, doi: 10.1177/13694332231191073.

[15] H.-J. Yu, S.-M. Kang, H.-G. Park, and L. Chung, 'Cyclic Loading Test of Structural Walls with Small Openings', *Int. J. Concr. Struct. Mater.*, vol. 13, no. 1, p. 40, Dec. 2019, doi: 10.1186/s40069-019-0352-1.

[16] C. P. Taylor, P. A. Cote, and J. Wallace, 'Design of slender reinforced concrete walls with openings', *Aci Struct. J.*, vol. 95, pp. 420–433, July 1998.

[17] T. P. Sah, A. W. Lacey, H. Hao, and W. Chen, 'Prefabricated concrete sandwich and other lightweight wall panels for sustainable building construction: State-of-the-art review', *J. Build. Eng.*, vol. 89, p. 109391, July 2024, doi: 10.1016/j.jobe.2024.109391.

[18] R. O'Hegarty and O. Kinnane, 'Review of precast concrete sandwich panels and their innovations', *Constr. Build. Mater.*, vol. 233, p. 117145, Feb. 2020, doi: 10.1016/j.conbuildmat.2019.117145.

[19] FIB Bullettin 74, 'Planning and design handbook on precast building structures'. 2014.

[20] R. Martins, R. D. Carmo, H. Costa, and E. Júlio, 'Load bearing capacity of connections between innovative pre-walls designed to have high durability and eco-efficiency', *J. Build. Eng.*, vol. 44, p. 103356, Dec. 2021, doi: 10.1016/j.jobe.2021.103356.

[21] V. T. Gerry and G. Alexander, 'Establishing Connection Methods for Precast Concrete Shear Wall', *Int. J. Eng. Tech.*, vol. 7, no. 1, Feb. 2021, doi: 10.29126/23951303/IJET-V7I1P8.

[22] R. Chang, N. Zhang, and Q. Gu, 'A Review on Mechanical and Structural Performances of Precast Concrete Buildings'.

[23] D. Kalliontzis and M. Nazari, 'Unbonded Post-tensioned Precast Concrete Walls With Rocking Connections: Modeling Approaches and Impact Damping', *Front. Built Environ.*, vol. 7, p. 638509, Apr. 2021, doi: 10.3389/fbuil.2021.638509.

[24] I. Arabi, 'BONDED AND UNBONDED POST- TENSIONING TECHNOLOGIES Post-Tensioning Systems In Building Construction', 2020, doi: 10.13140/RG.2.2.27638.14401.

[25] M. J. N. Priestley, S. (Sri) Sritharan, J. R. Conley, and S. Stefano Pampanin, 'Preliminary Results and Conclusions From the PRESSS Five-Story Precast

Concrete Test Building', *PCI J.*, vol. 44, no. 6, pp. 42–67, Nov. 1999, doi: 10.15554/pcij.11011999.42.67.
[26] S. Pampanin, 'Introduction to PRESSS-Technology'.
[27] G. Wang, Y. Li, Z. Li, and J. M. Ingham, 'Experimental and numerical study of precast concrete columns with hybrid bolted splice connections', *Structures*, vol. 28, pp. 17–36, Dec. 2020, doi: 10.1016/j.istruc.2020.08.042.
[28] F. Zhao, F. Xiong, G. Cai, H. Yan, Y. Liu, and A. Si Larbi, 'Performance and numerical modelling of full-scale demountable bolted PC wall panels subjected to cyclic loading', *J. Build. Eng.*, vol. 63, p. 105556, Jan. 2023, doi: 10.1016/j.jobe.2022.105556.
[29] M. Acharya, M. Acharya, K. Gurung, T. G. Wakjira, and M. Mashal, 'Seismic performance of full-scale modular structural concrete insulated panel walls with socket connection', *Innov. Infrastruct. Solut.*, vol. 10, no. 6, p. 211, June 2025, doi: 10.1007/s41062-025-02007-9.
[30] B. Cheng, Y. Cai, and D. T. W. Looi, 'Experiment and numerical study of a new bolted steel plate horizontal joints for precast concrete shear wall structures', *Structures*, vol. 32, pp. 760–777, Aug. 2021, doi: 10.1016/j.istruc.2021.03.043.
[31] H. Balineni, D. C. K. Jagarapu, and A. Eluru, 'Analysis of dry and wet connections in precast beam-column joint using ABAQUS software', *Mater. Today Proc.*, vol. 33, pp. 287–295, 2020, doi: 10.1016/j.matpr.2020.04.073.
[32] X. Chong, L. Xie, X. Ye, Q. Jiang, and D. Wang, 'Experimental Study on the Seismic Performance of Superimposed RC Shear Walls with Enhanced Horizontal Joints', *J. Earthq. Eng.*, vol. 23, no. 1, pp. 1–17, Jan. 2019, doi: 10.1080/13632469.2017.1309604.
[33] Z. Zhang and Y. Zhang, 'Research status on reinforcement connection form of precast concrete shear wall structure', *IOP Conf. Ser. Mater. Sci. Eng.*, vol. 322, 2018, doi: 10.1088/1757-899X/322/4/042001.
[34] Y. Lu, L. Jiang, and F. Lin, 'Seismic performance of precast concrete shear wall using grouted sleeve connections for section steels reinforced at wall ends', *Structures*, vol. 57, p. 105068, Nov. 2023, doi: 10.1016/j.istruc.2023.105068.
[35] W. Xue, Q. Huang, and Y. Li, 'Experimental study of precast concrete shear walls with spiral-confined lap connections under cyclic loads', *J. Build. Eng.*, vol. 52, p. 104467, July 2022, doi: 10.1016/j.jobe.2022.104467.
[36] A. Brandão *et al.*, 'Experimental characterization of the monotonic and cyclic behaviour of a new dry-horizontal joint between precast walls', 2025.
[37] 'ECCOMAS Thematic Conference'.

[38] R. Martins and R. Sousa, 'Performance of dry connections between precast concrete walls under monotonic shear loading'.

[39] *SAP2000*. (Copyright © Computers & Structures, Inc., -2016 1978).

[40] Vecchio, F. J. and Collins, M. P., 'The modified compression-field theory for reinforced concrete elements subjected to shear', *ACI J. 83.2*, pp. 219–231, 1986.

[41] Tsoukantas, S. G. and Tassios, T. P., 'Shear resistance of connections between reinforced concrete linear precast elements', *Struct. J. 863*, pp. 242–249, 1989.